RESERVE D5.3 v1.0

Report on field trial of voltage control concepts in Ireland and validation of initial network codes and ancillary service definitions

The research leading to these results has received funding from the European Union's Horizon 2020 Research and Innovation Programme, under Grant Agreement no 727481.

Project Name	RESERVE
Contractual Delivery Date:	30.09.2019
Actual Delivery Date:	06.10.2019
Contributors:	RWTH, TSSG, ESB, UCD
Workpackage:	WP5 – Test-beds for validation of research results
Security:	PU
Nature:	R
Version:	1.0
Total number of pages:	78

Abstract:

This document details the delivery of field trials of voltage control concepts developed in RESERVE at locations in Ireland.

Keyword list:

Smart Grid, Field Trials, Active Voltage Management, Virtual Output Impedance, Reactive support, Voltage Control Concepts, Volt-var curve, Impedance Measurement, Inverter, Solar PV, Battery Systems, Air Source Heat Pump, Vehicle to Grid.

Executive Summary

This deliverable detail the successful delivery of field trials of voltage control concepts developed in the RESERVE project through the realisation of those concepts in the field in parallel with the validation of new Network Codes and Ancillary Service proposals.

With regard to the Dynamic Voltage Stability Monitoring (DVSM) technique, the trials implemented the technique developed by RWTH through the development and testing of a prototype wideband-frequency grid impedance measurement device. The prototype was tested firstly in the laboratory in Aachen where the testing and uncertainty evaluation of the device was completed. Following this, field trails of the device were undertaken in Dublin, Ireland on October 2, 2019. During the trials, 52 experiments were conducted during which the inverter injected PRBS modulated current into the grid and the grid voltage was recorded. Based on the injected current and voltage at the point of common coupling, the grid impedance spectrum was extracted. Results from the simulations and the hardware prototype experiments in the form of lab trial and field trials validated the following proposed network codes;

- NC.14 Decentralised Voltage Control
- NC.15 Requirements for new behaviour of RES inverters
- NC.16 New requirements for the perturbations injected from RES inverters
- NC.17 Dynamic Stability Margins
- NC.18 Leading Power Factor Operation

With regard to the Active Voltage Management (AVM) control technique, six field trials in Ireland were developed in order to evaluate the performance of the technique. These trials incorporated four types of inverter based DER technology, namely Solar PV, V2G Charger, Domestic Scale Battery Storage Systems and Controllable Air Source Heat Pumps in order to implement the control technique and associated network services. For each trial site a combination of technologies and components, both hardware and software, were required from an ICT and Communications perspective to enable the deployment and facilitate the assessment and monitoring of the Active Voltage Management control technique. These deployments were undertaken whilst being cognisant of interoperability and scalability factors. In order to explore a new business model for AVM delivery a number of the trials sites utilised infrastructure owned and operated by a commercial aggregator to demonstrate a means by which to rapidly and cost effectively scale implementation of the technique. The implementation of the trails also served to facilitate the successful mass deployment of innovative Secondary Substation Sensors which served to both validate field trial performance and provide a solution for the real-time monitoring of Low Voltage (LV) networks. The performance of the trials were individually monitored and analysis completed on both the performance of the AVM Control technique and associated systems and software. The field trials succeeded in validating the AVM control technique in addition to validating the implementation of new ICT Architectures, business models and the following proposed network codes;

- NC.14 Decentralised Voltage Control
- NC.18 Leading Power Factor Operation

Authors

Partner	Name	e-mail
RWTH		
	Sriram Gurumurthy	sgurumurthy@eonerc.rwth-aachen.de
	Padraic McKeever	pmckeever@eonerc.rwth-aachen.de
	Antonello Monti	amonti@eonerc.rwth-aachen.de
TSSG		
	David Ryan	dryan@tssg.org
	Miguel Ponce de Leon	miguelpdl@tssg.org
	Niall Grant	ngrant@tssg.org
	Darren Leniston	dleniston@tssg.org
ESB		
	Ronan Murphy	ronan.murphy@esb.ie
	Tom Clancy	tom.clancy2@esb.ie
	Jonathan Sandham	jonathan.sandham@esb.ie
UCD		
	Alireza Nouri	alireza.nouri@ucd.ie
	Alireza Soroudi	alireza.soroudi@ucd.ie
	Andrew Keane	andrew.keane@ucd.ie

Table of Contents

1. Introduction

1.1 Scope of the Deliverable

RESERVE focuses on the energy systems at the system level, based on novel research concepts virtualising the control of power networks and on the use of a ground-breaking new pan-European real time simulation platform for the large-scale simulation of potential new solutions.

The document D5.3 is the third deliverable associated with the delivery of Field Trials for Voltage Control Scenarios within the RESERVE project and builds upon the findings in D5.1 and D5.2. It contains information about the design, installation, commissioning, execution and operation of the field trial sites in Ireland.

This document outlines the methods, concepts and achievements from completing task 5.2. Task 5.2 took elements of the ancillary services and network codes identified in Task 5.1 for validation and validated a selection of them across various trail sites. The task utilised field trial infrastructure developed by both project partners and third parties in order to capture and unearth the intricacies of operating a global voltage preservation platform across the entire electricity value chain.

1.2 How to read this Document

Before reading this document, the reader should read the document D1.1 which motivates the RESERVE project, describes the architecture of the RESERVE system and describes the RESERVE proposition, which instantiates the various architectures. We will avoid repeating detailed descriptions, which may be found in D1.1, D1.4 and D1.6.

Furthermore, in order to obtain a deeper understanding of the Voltage Control Techniques developed in the RESERVE project, deliverables associated with WP3 should be consulted in depth, in particular deliverables D3.3, D3.4 and D3.5 which detail the development of both the DVSM and AVM techniques.

In previous deliverables, the trial based on DVSM technique has been referred to as VOIP trials. However, this was according to the old plan in the project where a high-power commercial inverter would be procured, which would enable trialling the VOI control. Due to very high costs, this plan was altered and RWTH decided to build a low power prototype. During the early design phase, RWTH invented a novel low power, mobile, non-invasive impedance measurement concept and therefore RWTH decided to build the prototype which can be used as an inverter and as the proposed Wideband-frequency Grid Impedance (WFZ) measurement device. RWTH was successful in developing the prototype and tested the device in Aachen Lab and then in the field in Dublin, Ireland. The proposed device can be operated as a conventional inverter with a DC power supply or also as the proposed WFZ device without a DC power supply and hence we refer the prototype as a hybrid inverter in this document.

1.3 Structure of the Deliverable

This deliverable combines contributions from all project partners involved with the implementation of voltage control field trials. In order to provide a coherent structure for the reader the deliverable has been structured based on the control technique under trial and the specific technologies deployed.

Chapter 2 explores the Dynamic Voltage Stability Monitoring (DVSM) Field Trials developed by RWTH Aachen which incorporate a newly developed hybrid inverter.

Chapter 3 details the Active Voltage Management trials conducted using currently available inverter-based technologies across various sites in Ireland. Each site is examined in turn through a standardised structure of

i. Background

ii. Infrastructure Deployed

iii. Communications

iv. Data Information Systems & Software

v. Tuning of AVM Algorithm to Specific Site

vi. Performance of AVM Algorithm

Chapter 4 provides overall conclusions regarding the successful deployment of the Field Trials.

2. Dynamic Voltage Stability Monitoring Trials

2.1 Introduction and Background

This chapter covers the invention of RWTH where a wideband-frequency grid impedance measurement device prototype is developed and tested. The prototype has been tested firstly in the laboratory in Aachen where the testing and uncertainty evaluation of the device was done. Following this, the device was trialled in Dublin, Ireland on October 2, 2019. During the trials, 52 experiments were conducted where the inverter injects PRBS modulated current into the grid and the grid voltage was recorded. Based on the injected current and voltage at the point of common coupling, the impedance spectrum was extracted.

2.2 Theory

To test the algorithms proposed in the scenario Dynamic Voltage Stability Monitoring (Sv_A), a new class of inverters are required. In the impedance-based approach undertaken in Sv_A, the measurement of grid impedance is a crucial step. A wideband system identification (WSI) tool is developed to measure and extract the grid impedance by injecting small signal perturbations in the control of the inverter. The process of procuring such new class of inverters which does not exist in the market, externally, was not cost effective. Therefore, RWTH has developed a new inverter with the proposed functionalities of WSI and virtual output impedance (VOI) control algorithms. During the early stages of development, RWTH invented a mobile concept for a device which can measure the grid impedance and perform stability monitoring in real-time. A patent is pending for this invention. The prototype of the inverter was tested in the lab in Aachen and also trialled with the Irish distribution grid in Dublin in coordination with ESB Networks.

The objective of the DVSM Irish field trial is to measure the grid impedance with the proposed prototype inverter and examine the quality of extracted impedance. Section 2.6 contains the results and analysis of the DVSM Irish field trial.

2.2.1 Impedance based stability for active distribution grids

The phenomenon of harmonic instability and parallel resonance has been mapped to the concept of impedance from the Middlebrook theory. The stability properties of a power-electronic driven system can be adjudged by the impedance ratio of the grid as seen from the converter and the converters impedance. Thus, the proposed Dynamic Voltage Stability Monitoring (Sv_A) technique starts from the impedance measurement process: the grid impedance as seen from the RES inverter needs to be measured. An online non-invasive technique based on Wideband System Identification (WSI) for the grid impedance measurement is reported in Deliverable D3.4. Real-time hardware-in-the-loop simulations show the effectiveness of the WSI technique to measure and estimate the grid impedance.

Based on this concept, a standalone mobile impedance measurement device is proposed. The proposed measurement device utilizes the Wideband System Identification (WSI) technique to measure the grid impedance at the point of common coupling. This technique injects PRBS signal which is superimposed over either the duty cycle, voltage or current reference signals of the device. One of the major applications for which the invented device is intended is shown in Figure 1. Consider a low voltage distribution feeder with arbitrary number of buses and let's assume that the stability margins at Bus 6 needs to be monitored as shown in Figure 1.

The device is connected at Bus 6 and performs impedance measurement using the WSI block by injecting perturbations in voltage and current. The voltage is measured at the PCC as shown by the red dotted line and the currents are measured on both sides of the red dotted line. Thus, the impedance of two sections of the LV feeder Z6L and Z6R with respect to the PCC can be measured by the proposed device. Based on the impedances Z6L and Z6R that are measured, the stability margins are calculated.

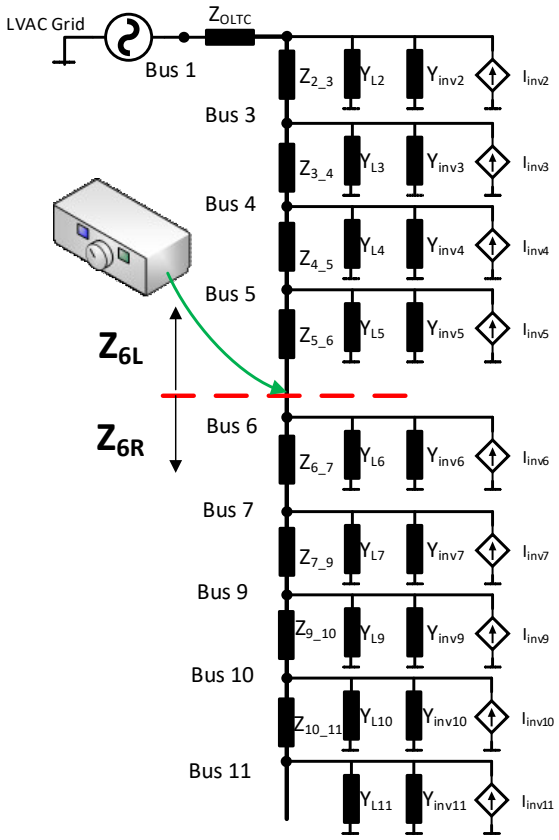

Figure 1: Stability Monitoring Concept for Active Distribution Grids

2.2.2 Virtual Output Impedance (VOI) Control

Closed loop impedance of the inverter is dependent on the control loops of the inverter. Modifying the controller changes the impedance of the converter. Control techniques in literature which try to modify the output impedance do not consider the real-time grid impedance. From the Middlebrook theory and its advancements, it is proved that the stability of every power electronic interface is dependent on the ratio of the grid impedance and inverter output impedance. The VOI technique proposed in WP3 considers the real-time grid impedance data for the synthesis of stabilizing VOI controller. [1] Real-time measurements of the impedance through the WSI tool enables the application of advance control techniques such loop-shaping techniques for the synthesis of VOI. Ultimately, the impedance of the inverter is modified to suit the measured grid impedance. Concept of VOI is illustrated in Figure 2. Details of the VOI controller and its synthesis can be found in Deliverable D3.5. Real-time simulations of the proposed VOI control can be found D5.7 and D3.9 and frequency domain stability analysis can be found in D3.9. Real-time simulations show that VOI controller can actively change inverters dynamic behaviour and damps the resonance which prevents the system from entering harmonic instability.

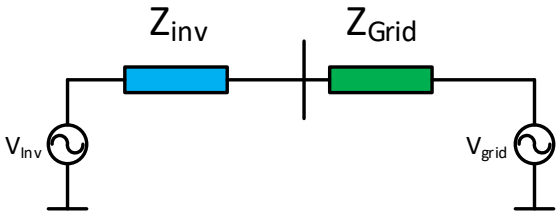

Figure 2: VOI Concept

2.2.3 Dynamic Voltage Stability Monitoring for Future Distribution Grids

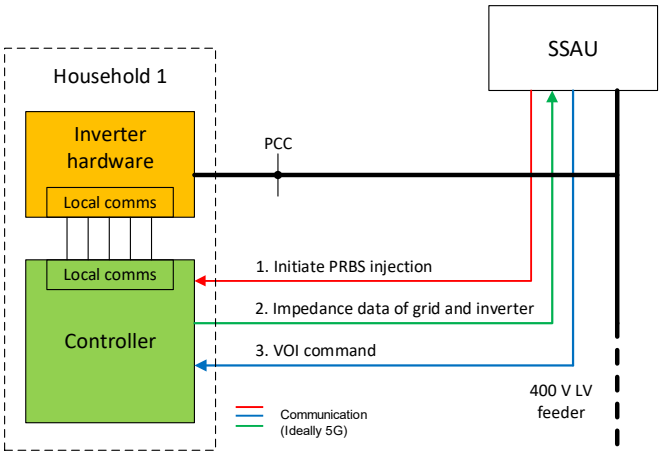

Figure 3: DVSM Technique

The three-step process of the DVSM technique as shown in Figure 3 can be summarised as follows. The first step is the initiate noise injection command from the SSAU to the inverter. Following which the inverter measures the grid impedance. The inverter calculates its output impedance coefficients from the mathematical model which is known to the inverter. In the second step, the inverter hardware communicates the grid impedance data and inverter output impedance data to the SSAU. Following which the SSAU calculates the dynamic stability margins and VOI command. The third step is where the SSAU communicates the VOI command back to the inverter. This completes 1 computation cycle of DVSM for 1 household, let's denote it as t_p seconds. This process is repeated for every household with RES inverter, one at a time. The time period t_p and the number of houses N under a given SSAU is a crucial factor in determining the number of cycles of DVSM (denoted by f_dvsm) that can be performed for a given LV distribution system in 1 hour. We envision that one cycle of DVSM cycle per household t_p takes about 0.5 to 0.7 seconds. Therefore, on an average considering 500 households under an SSAU, we envision the DVSM cycle for this portion of the distribution grid can be completed in 300 seconds. Therefore, the number of cycles of DVSM for the distribution grid in an hour is roughly 12 to 14 cycles.

2.3 Wideband Grid-frequency Impedance Measurement (WFZ) Device

2.3.1 Setup

The new device proposed is shown in Figure 4 within the encapsulated box, where the hardware part is highlighted in yellow and the software part is highlighted in green. The device consists of a 3-phase converter with B6C topology and power electronic switches can be realized with either IGBTs or MOSFETs based on the voltage level and carrier switching frequency. The DC side of the converter consist of a negative temperature coefficient (NTC) resistor, relay and a DC link capacitor. The AC side consists of a LCL filter and a relay. In the software side, a controller which could either be conventional current control or non-linear control synthesizes the control command for the PWM block which controls the switching of the IGBTs. The controller relies on measurement of grid injected current, grid voltage and the voltage of the DC link capacitor.

A wideband system identification (WSI) and information management block interacts with the controller. The WSI block is further enabled with communication to communicate the measured grid impedance data to the Secondary Substation Automation Unit (SSAU) for further monitoring.

2.3.2 Method

The DC link capacitor is charged from the grid by closing the DC side relay. The NTC resistor limits the inrush current during start-up. During this period, the B6C bridge is operated as a rectifier. Then, the stored energy is injected back into the grid and the B6C bridge is operated as an inverter. During this time, the WSI block injects PRBS noise signals into the current reference of the inverter for 40ms (2 cycles of fundamental grid voltage). Simultaneously, the voltage and current signals are measured and stored in first-in-first-out (FIFO) buffer. The grid impedance is calculated in frequency domain using fast Fourier transform (FFT) algorithm and system identification technique is applied to get the impedance transfer function. The measurement of impedance can be done either in direct-quadrature (DQ) domain or in sequence domain based on the requirement. The device can then compute stability margins by applying impedance-based stability assessment techniques. The device can communicate the identified grid impedance coefficients and the calculated stability margins to the SSAU, where corrective steps are undertaken.

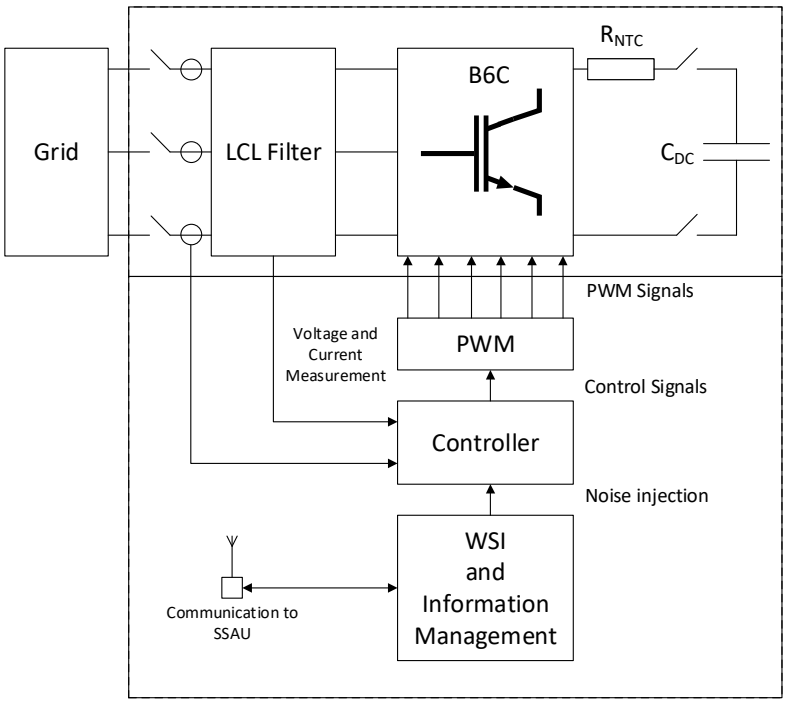

Figure 4: Structure of the proposed measurement device (WFZ device)

The proposed device does not require any external power supply since it takes power from the grid and injects back into the grid during measurement. The amount of power consumed is negligible compared to devices which incorporate load switching. The device need not be rated for high power since the goal is to inject small signal perturbations in the grid. Because of the above-mentioned reasons, the device is low cost, low weight and mobile. The envisioned device has high plug-play capability for distribution grid operators to plug the device at any node along the low voltage distribution feeder and measured impedance in real-time and have the stability monitoring executed in real-time. The envisioned device will be equipped with communication capabilities to relay the information to the SSAU. Furthermore, disturbance injected in the grid is negligible since the device is based on WSI concept which is a small-signal technique.

2.4 Trial Site Implementation

2.4.1 Hybrid inverter prototype development

The parameters of the constructed hybrid inverter are shown in Table 1.

Converter Parameters	Values
DC Link Voltage	600-750 V
Grid Voltage and Frequency	400 V, 50 Hz
Switching Frequency	50 kHz
Converter Side Choke	2.7 mH, 0.5 Ω
Grid Side Choke	1.8 mH, 0.3 Ω
Filter Capacitance Co	1 μF

Table 1: Hybrid Inverter Parameters

2.4.1.1 Inverter and power filter board

PCB of the main inverter board is shown in Figure 5. The semiconductor switches and the gate drive logic are realized from the intelligent power module (IPM) technology-based integrated circuit FSBB20CH120D by ON Semiconductors. Considering an operating power of 300W, the inverter can be operated with a switching frequency of 50 kHz. However, when the inverter needs to be operated at a much higher power, then the switching frequency can be reduced to 20 kHz or 15 kHz to be in safe operating mode. This IPM offers inbuilt short circuit current protection and galvanic isolation. The control signals that drive the PWM and relays are provided from the Labview NI FPGA controller. Digital isolator ICs are incorporated in the design to galvanically isolate the Labview NI FPGA from the high voltage side.

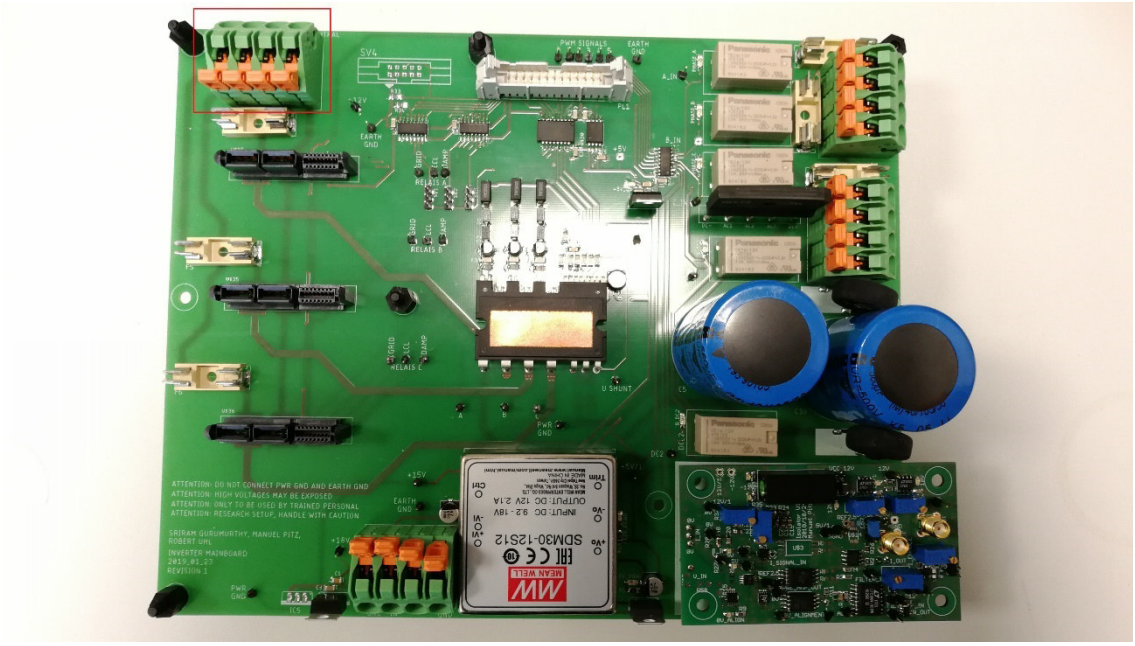

Figure 5: Main Inverter Board

The power filters are realized with an LCL filter with split RC damper to supress the filter resonance. Relays are included to configure the power filter (i.e. LC or LCL) and to configure the shunt damper. The cut off frequency of the LCL filter is designed to be roughly one tenth of the switching frequency. Since the inverter is planned to be operated at 50 kHz, the cut off frequency of the realised filter is 5.01 kHz. A split capacitor damping topology is realized for the passive damping circuit. Objective of the damper is to remove the resonance peak introduced by the LCL filter at its cut-off frequency. PCB of the realized filter board is shown in Figure 6.

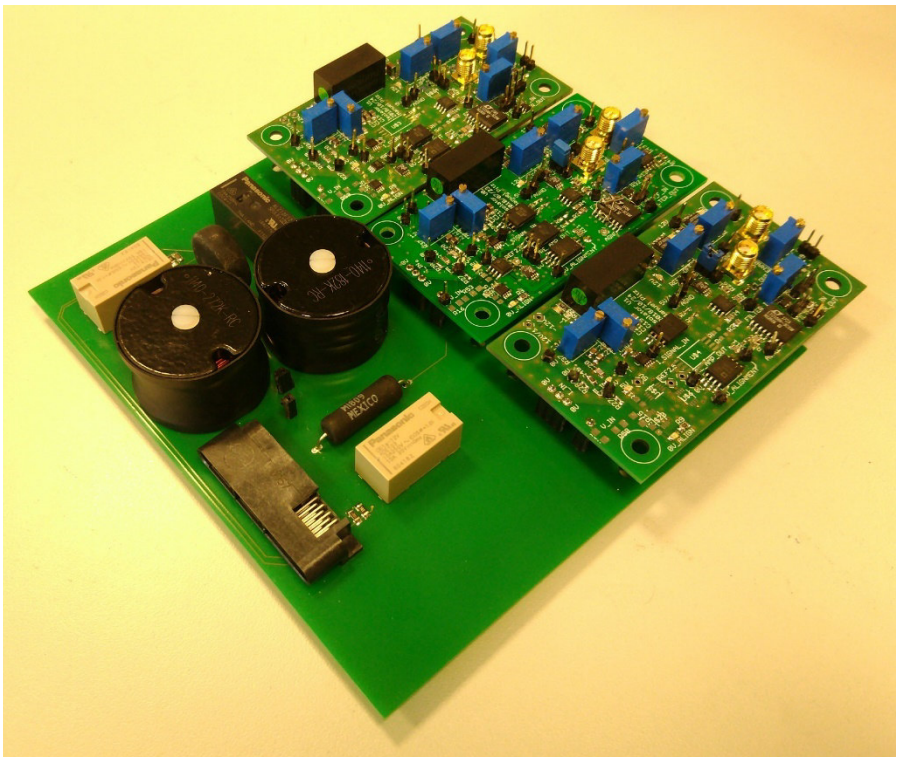

Figure 6: Reconfigurable LCL Filter Board

2.4.1.2 Measurement board

The measurement board developed have adjustable bandwidth and offer excellent resolution on the measured voltage/current. Galvanic isolation of 1 kV is guaranteed by this board and implements an 8th order low pass filter to strongly attenuate noise. All the boards were auto-calibrated on the fly during the start-up sequence of the control software, which eliminates errors such as offset and wrong gain. Measurement board PCB is shown in Figure 7.

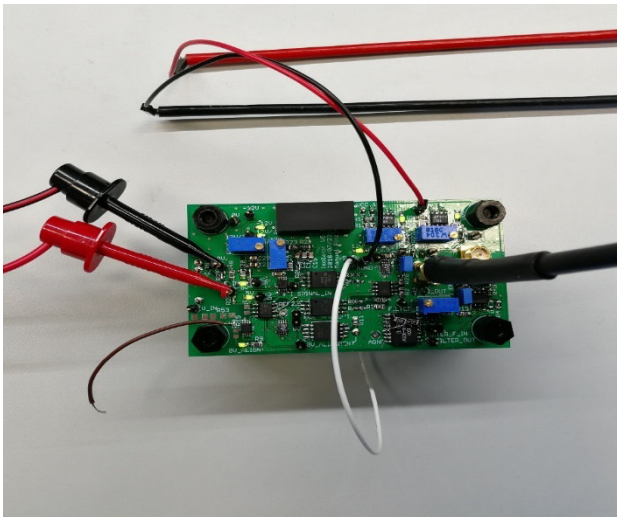

Figure 7: High bandwidth current and voltage measurement board

2.4.1.3 Overall Design

Three filter boards are stacked on the main inverter board in a perpendicular manner. Measurement boards to measure current or voltage in each phase are stacked onto the corresponding filter board. Such a modular design allows easier replacement and repair when a fault occurs and furthermore reduces the space. Since the inverter was shipped back and forth from Aachen, Germany to Dublin, Ireland, designing an inverter which can be disassembled and assembled was required. Space reduction in the design was also important to cut down on shipment costs. The total development cost for this prototype is around 1500 – 2000 EUR.

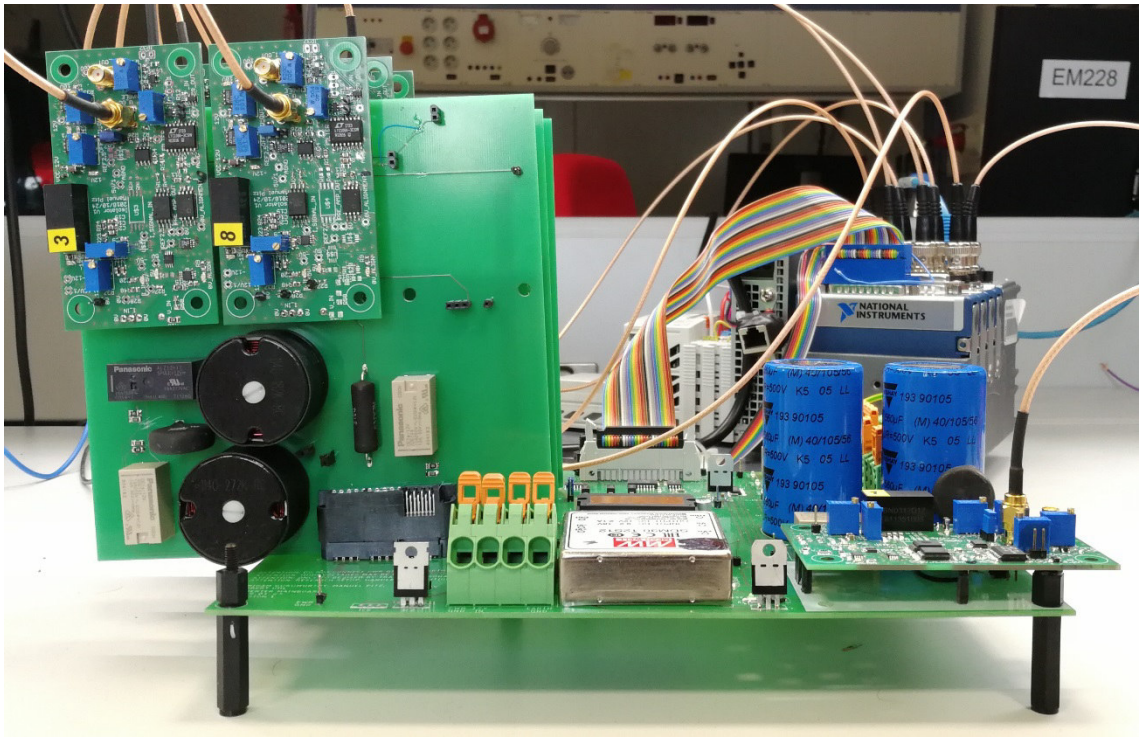

Figure 8: WFZ Device Prototype

2.4.1.4 Control Algorithm

The control algorithm is implemented in a Labview real time FPGA target. The control algorithm in the inverter can be grouped in 2 parts: **Operation&Control** and **Impedance measurement**.

Operation&Control: A cascaded proportional-integral (PI) control is implemented for controlling the grid injected current. Additionally, the proposed VOI loop is included in into the cascaded structure. This group also contains all the signals to operate the relays.

Impedance Measurement: Contains the WSI tool and its components such as FIFO buffer for data acquisition.

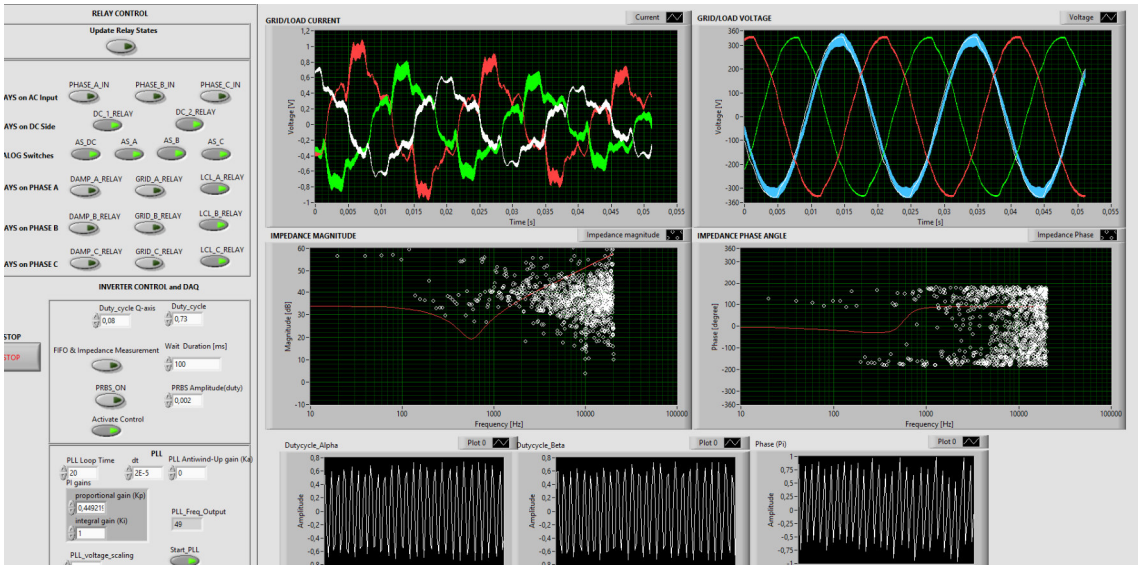

Figure 9: Front Panel - Labview Inverter Control Software

2.4.2 ESB Trial Site Preparation

ESB prepared a trial location in Engineering Centre Lab at UCD. A three phase IP44 socket (with 3 phase wires, neutral and ground) and a suitable cable was prepared for the connection of prototype three phase inverter. A controlled rectifier capable of operating at 650 to 750 V DC was used as the DC power supply for the prototype. A 4-channel high bandwidth oscilloscope was provided to verify the phase synchronism between the inverter and the grid before initiating the connection to the grid. Furthermore, a low voltage power supply capable of supplying 18 V DC was prepared at the trial site which is used for powering up the low voltage functionalities in the inverter such as operation of measurement boards and relay circuits.

Since the high voltage DC power supply, which is in this case a controlled rectifier, emits high EMI, it was noticed that this EMI affects the inverters functionality. Therefore, it was decided to operate the inverters DC link at a much lower voltage. A star-delta 380V/178V transformer was provided to reduce the point of common coupling (PCC) voltage to roughly half the grid voltage. Thus, the inverter was operated with a DC link voltage of 300-350 V range instead of the conventional 600 to 700 V range.

2.5 Aachen Lab Trial - Results and Analysis

2.5.1 Aachen Lab Trial – Grid Forming Mode

The WFZ device is operated with a DC Link voltage and it is operated in grid forming mode. A three-phase passive impedance network is sued as the load impedance that needs to measure similar to the simulations performed previously. The device is operated at 50 kHz and the noise injection is also performed at maximum possible frequency of 50 kHz. Considering a N-bit shift register to generate the noise, we need $2^N - 1$ sample points. In the simulations and experiments, it was found that N=11, is a sufficient choice for obtaining sufficient frequency resolution, thus leading to 2047 sample points. At 50 kHz and N=11 bits, the measurement time period for measuring d-axis impedance is 40.9 ms. Between d-axis and q-axis impedance measurements, a dead-time of 0.02 seconds (1 cycle of power system frequency) is observed for the transients to settle down. Q-axis impedance requires another 40.9 ms. Thus, the total measurement time for measuring DQ impedance matrix is 0.101 s.

Figure 10 shows the load current and Figure 11 shows the load voltage during the perturbation window of 0.101 s. The obtained d-axis impedance magnitude and phase are plotted in Figure 12 and Figure 13. In order to validate the obtained measurements, a network analyser is used to make a reference measurement which is denoted by the red line in Figure 12 and Figure 13.

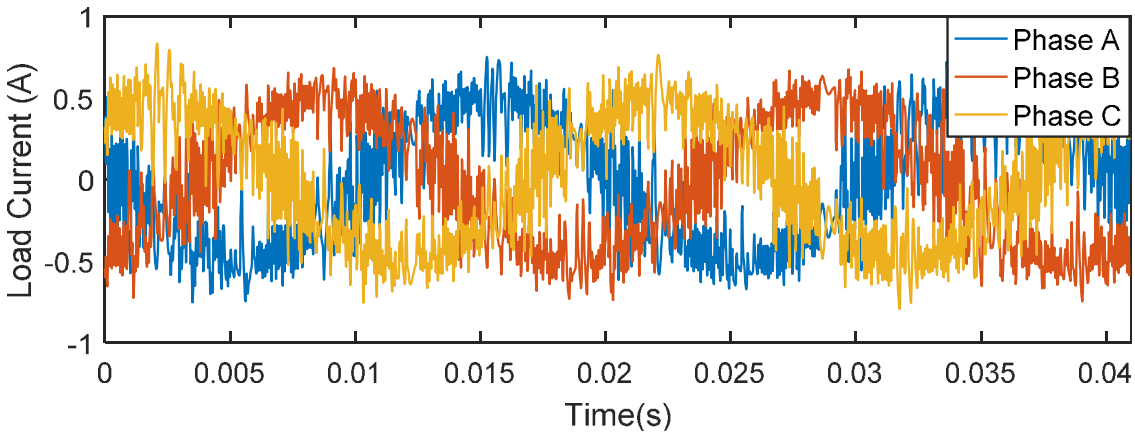

Figure 10: Load Current

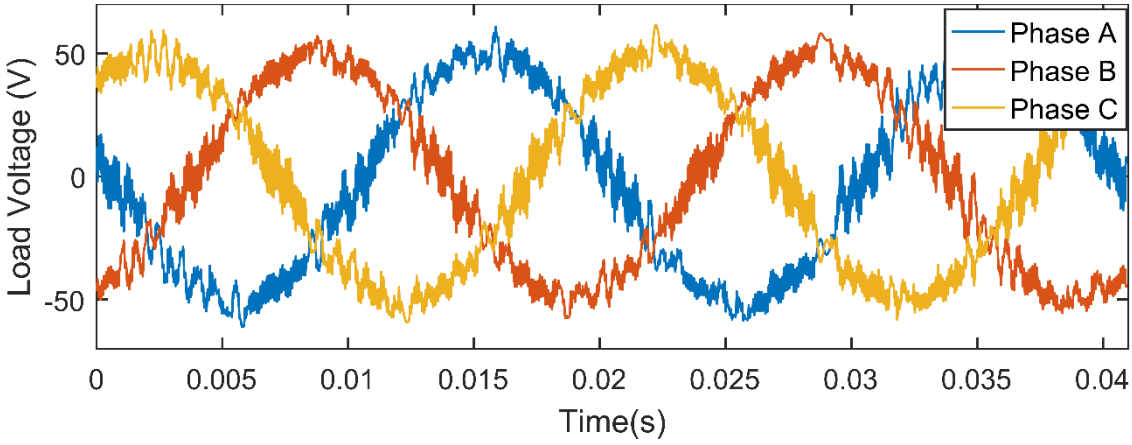

Figure 11: Load Voltage

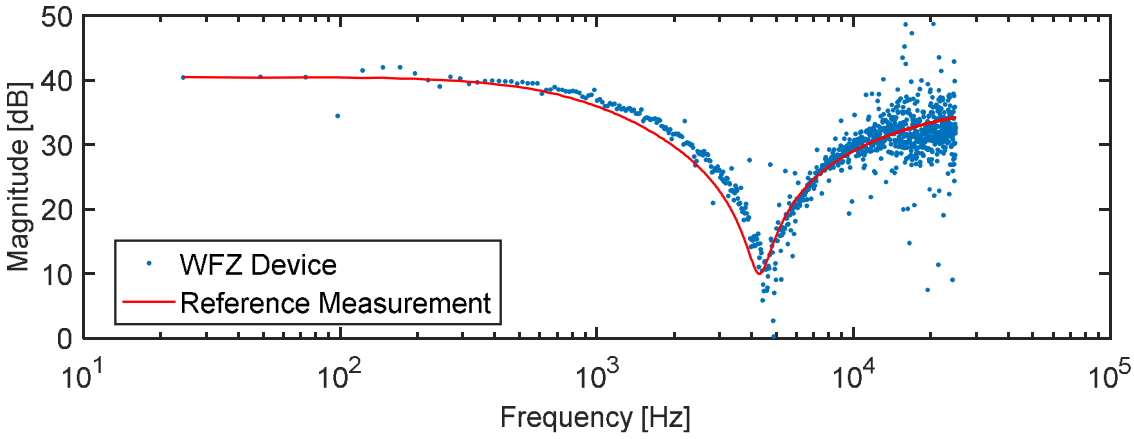

Figure 12: D-axis Impedance - Magnitude

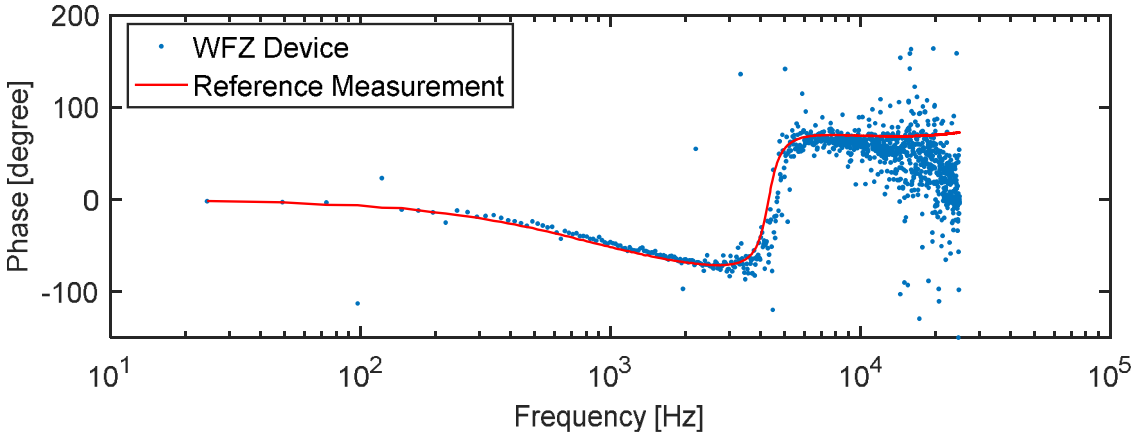

Figure 13:D-axis Impedance – Phase

Wideband grid impedance measurement is a novel concept for power grids and currently no such wideband frequency grid impedance measurement devices exist in the market. The accuracy of the overall device depends on the accuracy of the voltage, current measurement units and Analog to Digital Converters (ADCs). A wideband grid impedance device is developed within RESERVE project for trialling in Aachen Lab and Irish grid.

Since wideband grid impedance is a complex number defined over a frequency grid, the accuracy of the impedance measurement can be evaluated by complex curve fitting techniques.

A known passive networks impedance is first measured using a highly accurate frequency analyser $Z_{m}(f_i)$ following which the impedance data points obtained from the impedance measurement device $Z_{act}(f_i)$ can be used to calculate the norm η defined in (2-1). Here N refers to the number of points in the frequency grid.

$$\eta = \frac{1}{N}\sum_{i=1}^{i=N}\left|\frac{Z_m(f_i) - Z_{act}(f_i)}{Z_{act}(f_i)}\right|^2 \quad (2\text{-}1)$$

About 50 experiments are conducted and the impedance deviation norm is calculated to determine the closeness of the measured impedance and reference impedance obtained from a high precision network analyser. Since the proposed device is highly accurate until 10 kHz, the impedance deviation norm is calculated until 10 kHz. The variation of η is presented in Figure 14. It can be observed that the device offers high precision since almost all the norm values are close to the mean. Figure 15 shows the normalized probability of the norm for the 50 experiments. The mean of the norm is 1.21 and the standard deviation σ is 0.03 which is indicative of high accuracy and precision of the device.

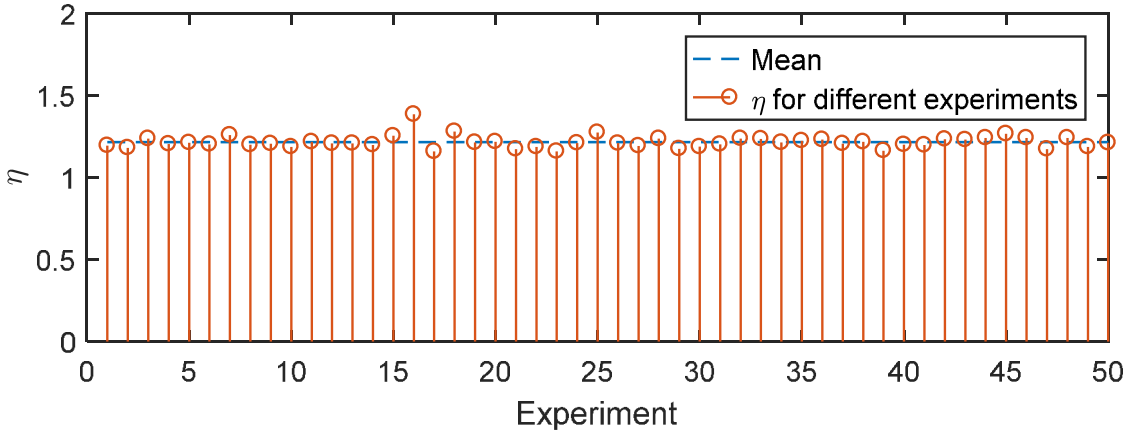

Figure 14: Variation of Impedance Deviation Norm

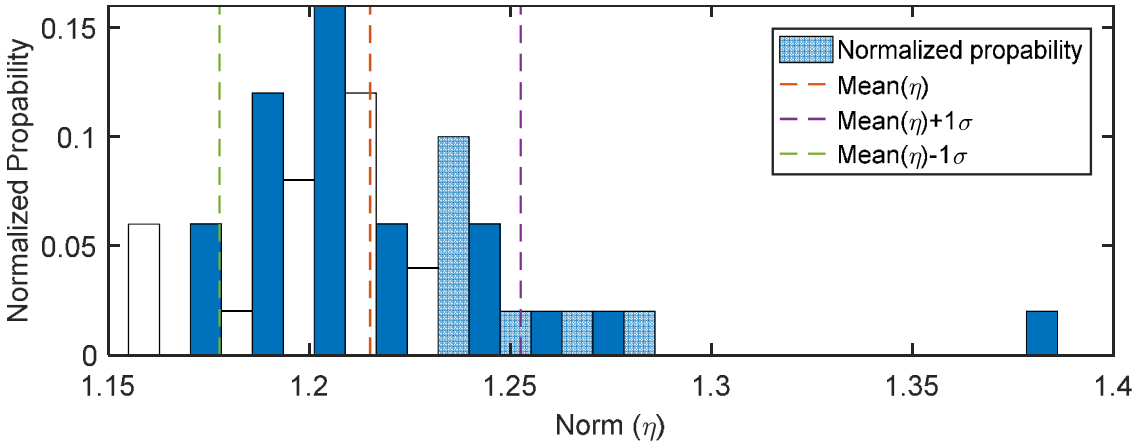

Figure 15: Uncertainty evaluation of WFZ device

2.5.2 Aachen Lab Trial – Grid Connected Mode

This section consolidates the testing and commissioning of the prototype inverter to operate in grid connected mode.

After trailing the inverter with a passive load rack, the DC link voltage was ramped up to 600-650 V to enable grid connection. The schematic for the lab trial in grid connected mode is shown in Figure 16. A 3-phase synchronous reference frame PLL (SRF-PLL) is designed to

synchronize the inverter output with the grid. Figure 17 shows the synchronized inverter output voltage (in blue) and the grid voltage (in yellow), wherein both magnitude and phase have matched.

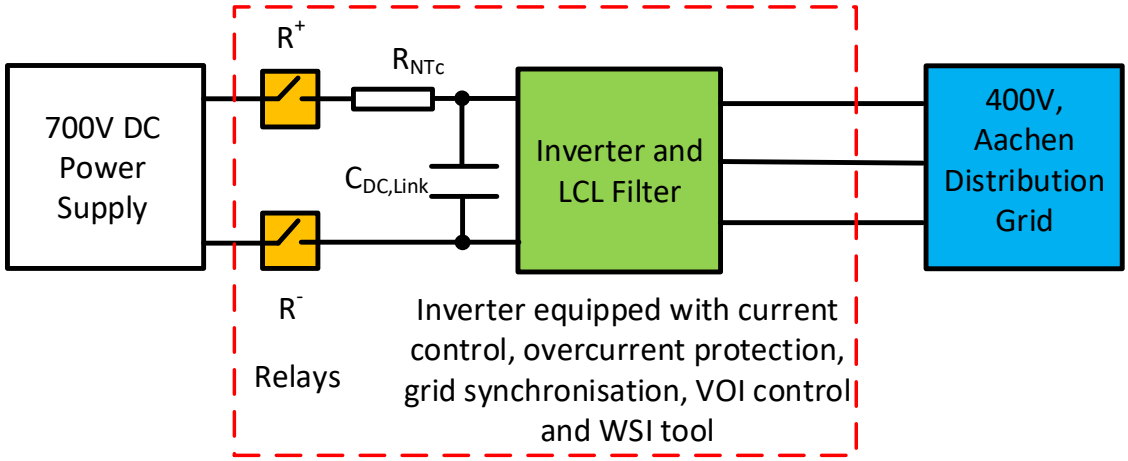

Figure 16: Aachen Lab Trial Setup - Grid Connected Mode

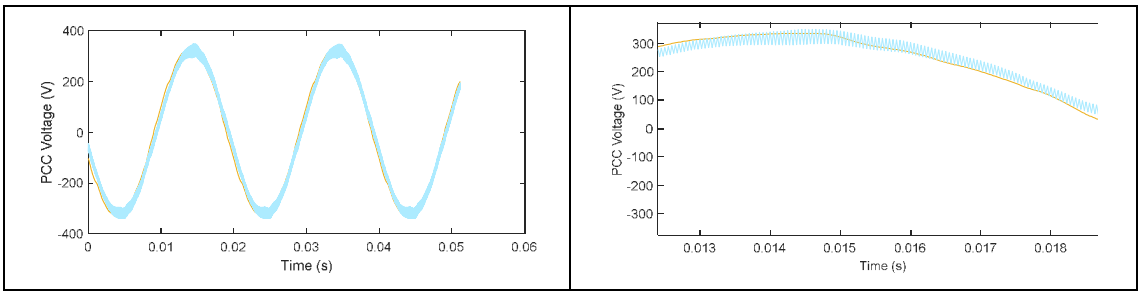

Figure 17: PLL Synchronization

PLL synchronization was ensured for all phases and the inverter output voltage and grid voltage were verified for matching phase sequence. Upon closing grid relays, the PCC voltage remains stable as shown in Figure 18. The inrush grid current is shown in Figure 19 which decays with time to be approximately zero. The peak value of inrush current is reduced by using NTC resistors at the output of the inverter. At this point, the inverter stays grid connected and stays stable without injecting any active or reactive power into the grid.

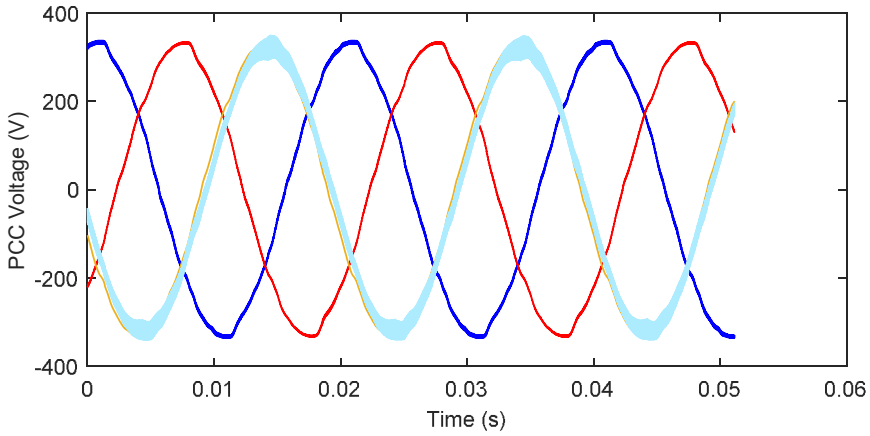

Figure 18: PCC Voltage

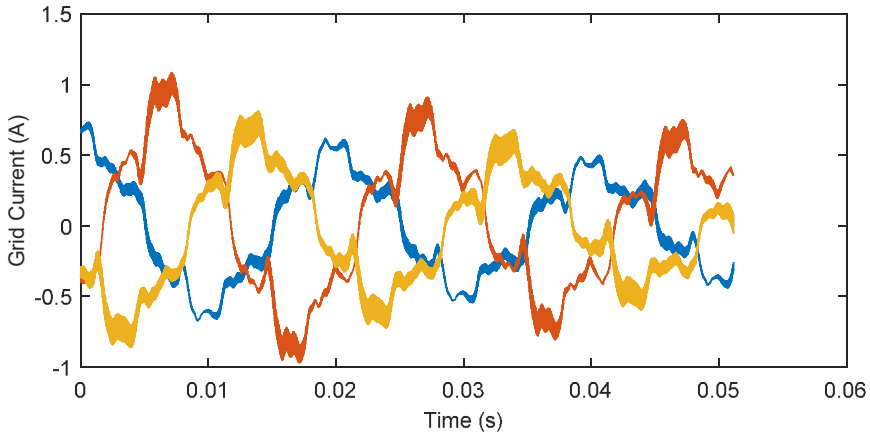

Figure 19: Grid Current

2.6 Irish Field Trial – Results & Analysis

2.6.1 Irish Field Trial Description

The field trials were conducted on October 2nd, 2019 in Dublin, Ireland.

The schematic of the Irish field trial is shown in Figure 20. A star-delta 380V/178V transformer was provided to reduce the point of common coupling (PCC) voltage to roughly half the grid voltage. Thus, the inverter was operated with a DC link voltage of 300-350 V range instead of the conventional 600 to 700V range. Due to the presence of the transformer, the measured impedance would be combination of the transformer impedance and grid impedance. Thus, from this experimentation standpoint, grid impedance would be referred to the impedance seen by the device which would be transformer plus the grid itself. A picture of the experimental setup is shown in Figure 21.

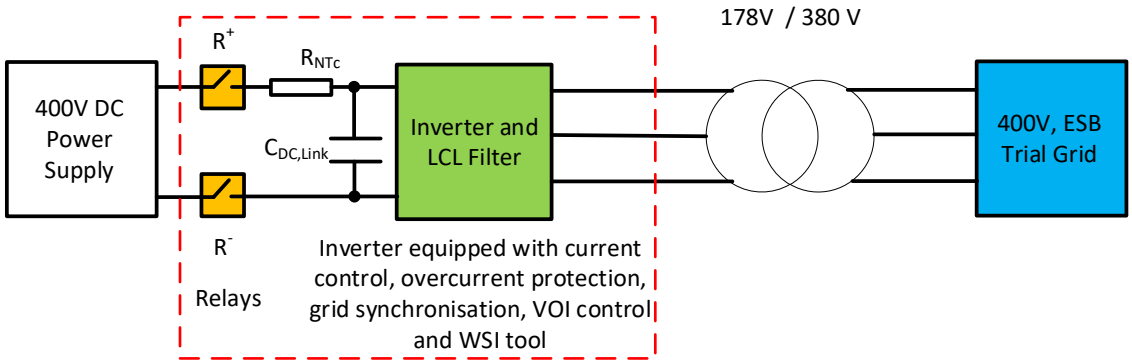

Figure 20: Irish Field Trial Setup

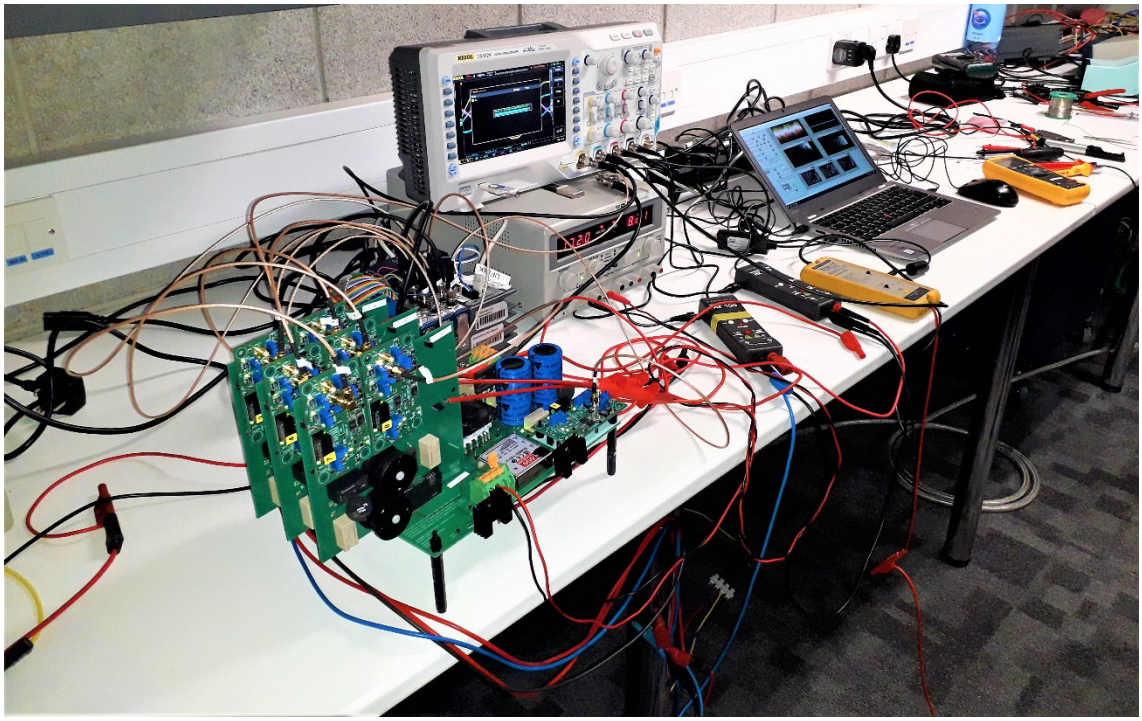

Figure 21: Experimental Setup of Irish Field Trial, Dublin

In an identical manner, as done in Aachen Lab trial – grid connected mode, the inverter was first synchronized on all phases using the SRF-PLL. Figure 22 shows the comparison of the inverter voltage with and without PRBS injection. During PRBS injection, the system remains locked with the grid and does not lose synchronism.

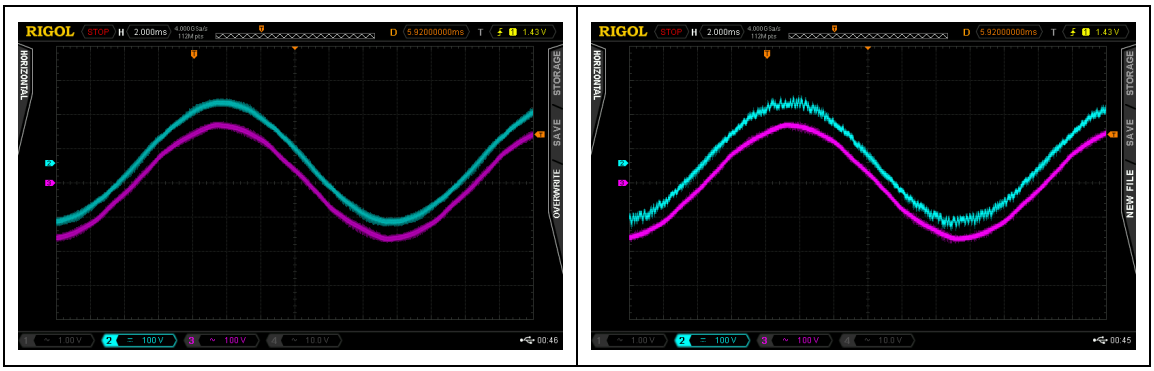

Figure 22: PLL Synchronization with and without PRBS injection

2.6.2 Results

The usage of step-down transformer enables a lower DC link voltage compared to conventional operation. The DC link remains stable during the injection period as shown in Figure 23.

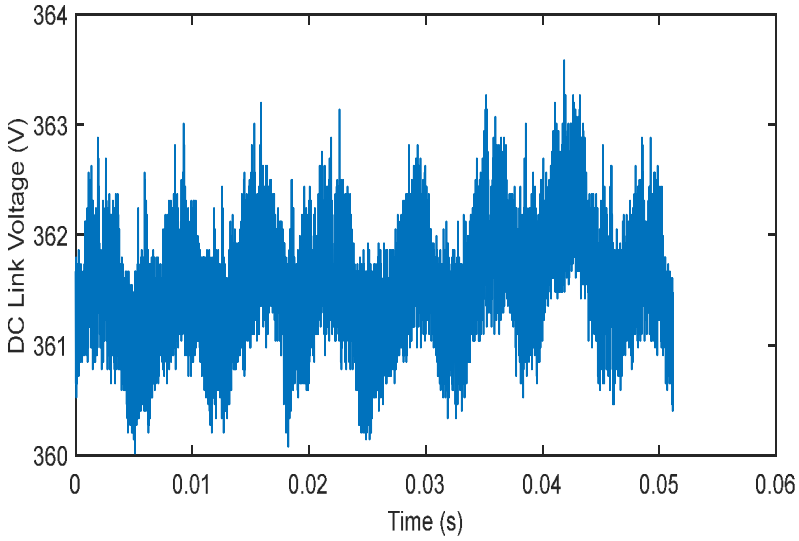

Figure 23: DC Link Voltage

The inverter was operated at 20 kHz due to operational constraints and stress on the IGBT. Section 2.5.1 covers the parameters of the PRBS signal to used. The PRBS injection is done at 20 kHz and the voltage/current samples were collected for 50 ms. Figure 24 shows the grid injected current and its corresponding spectrum. PRBS modulated currents are injected up to 5 kHz after which the filter strongly attenuates the currents.

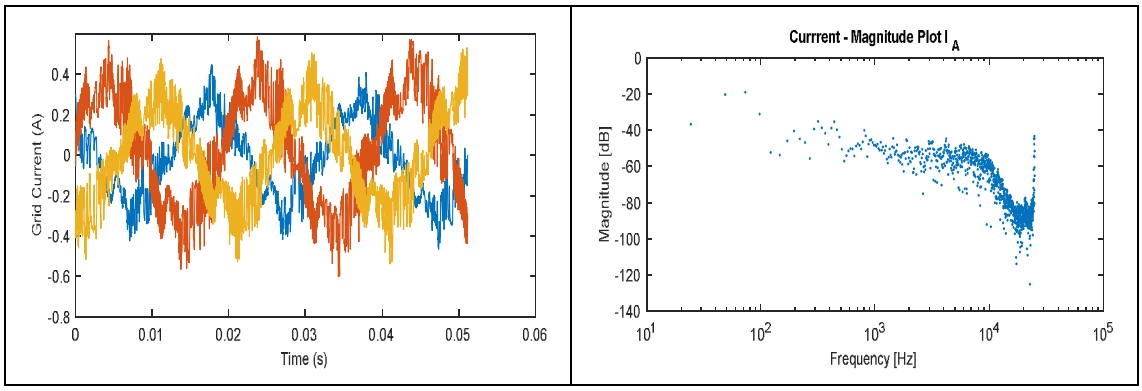

Figure 24: Grid Current and its Spectrum

Figure 25 shows the grid voltage measured at the PCC and its spectrum, it can be noticed that the grid is not perturbed by the injected current, meaning that the grid is a strong grid. Only a weak grid, which has larger impedance would get perturbed in a noticeable extent. From the output voltage and current spectrum the impedance is calculated.

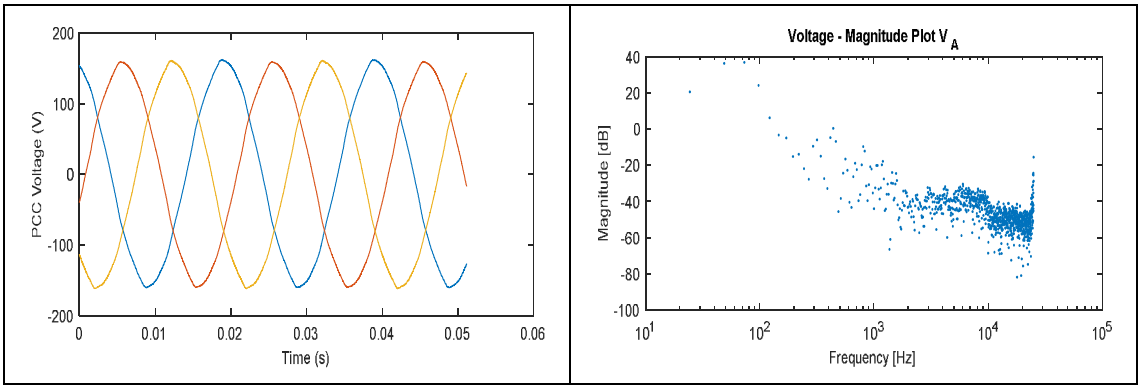

Figure 25: PCC Voltage and its Spectrum

Figure 26 Figure 27 show the spectrum of the extracted grid impedance. Around 52 experiments were performed, during which the PRBS levels were gradually increased. It was noted that the grid does not get perturbed due to its very low to zero impedance. It was noticed that the quality of extracted impedance improves as the PRBS levels are increased. However, for effective validation, measurements in a Microgrid will be interesting and measuring with a grid emulator where a certain grid impedance is emulated would be suitable. The device was able to extract the impedance in the low frequency ranges.

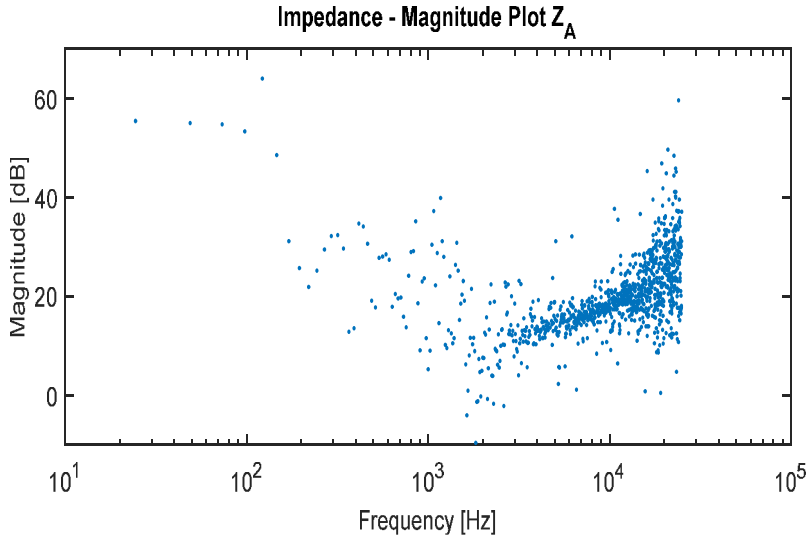

Figure 26: Grid Impedance Magnitude Spectrum

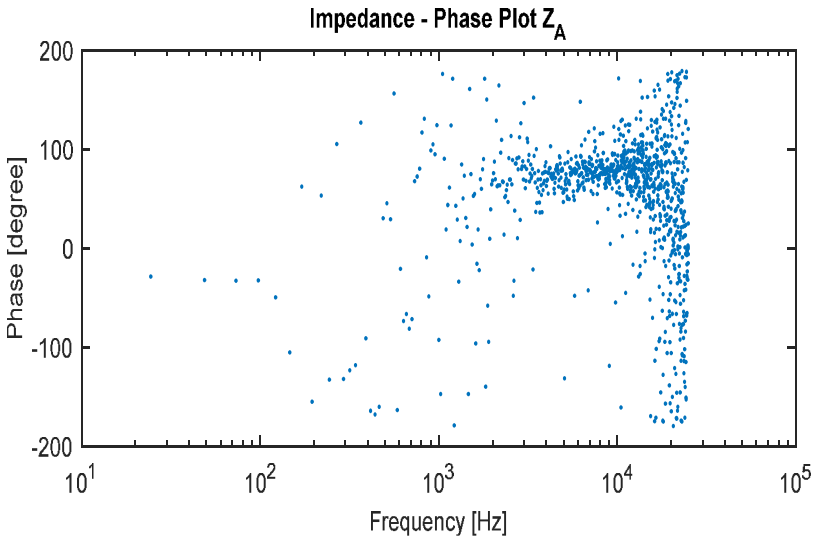

Figure 27: Grid Impedance Phase Spectrum

2.6.3 Verification of Grid Codes

- The Irish trials and Aachen lab trials successfully verify the network code **NC. 16 New requirements for perturbations injected from RES inverter**. PRBS injections are vital for future converter system to have an inbuilt diagnostic and monitoring tool since grids are transforming to be weak due to high penetration of volatile energy sources.
- As an outcome of the measured impedance from the WFZ device, stability can be analyser from the non-parametric Nyquist plots and thus we propose **NC. 17 Dynamic stability margins**. Details regarding the application of stability criterion and the device itself is given in D3.3 and D3.8.

- Virtual output impedance control proposed in RESERVE is a novel concept where the stability is ensured by design. The grid impedance measured is augmented in the inverter model to synthesise an appropriate VOI controller, thereby guaranteeing stability. The proposed method is validated via real-time simulations using the OPAL-RT real time simulator. The results of the real-time simulation can be found in D5.7 and D3.9. The proposed method can mitigate an inverter from entering into harmonic instability. Thus, we have validated the recommended network code **NC. 15 Requirements for new behaviour of RES inverters.**

2.7 Conclusion

This chapter consolidates the work on Dynamic Voltage Stability Monitoring technique. DVSM technique is a 3-step process which consists of an impedance measurement concept, an impedance-based stability monitoring concept and an impedance based decentralised voltage control concept. RESERVE has developed strong theoretical foundation on the above-mentioned concepts.

RESERVE has developed a non-invasive wideband system identification (WSI) tool which can measure the grid impedance for wide range of frequency in a short time without interrupting the grid. Offline and hardware-in-the-loop simulations have validated the proposed concept in D3.4. Generalized Nyquist Criterion (GNC) has been identified to be the most suited tool for stability of three phase AC systems. For applying GNC, the impedance of the inverter and grid is required. Grid impedance can be acquired using the WSI technique and the inverter impedance can be analytically modelled. D3.3 applies the proposed stability criterion for the Irish distribution grid and has validated the generic effects of cable length, converter bandwidth etc. on stability margins when under high RES penetration. RESERVE adopts the stability by design philosophy and ha addressed a solution for future converter-based system using the virtual output impedance control. RESERVE proposes a generalised framework for the synthesis of VOI control using the measured grid impedance. Validation of the VOI technique was undertaken through offline simulations in D3.5, frequency domain stability analysis in D3.9 and though real-time simulations in D5.7.

Due to high costs involved in procuring a customized inverter with such advanced functionalities, RWTH decided to build a low power inverter prototype. During the early design phase, RWTH invented a novel low power, mobile, non-invasive impedance measurement device and therefore RWTH decided to build the prototype which can be used as an inverter and as the proposed Wideband-frequency Grid Impedance (WFZ) measurement device. RWTH was successful in developing the prototype and tested the device in Aachen Lab during which the device was accurately and precisely calibrated. Uncertainty evaluation of the device was done for the characterization and ascertainment of future measurements. The proposed device can be operated as a conventional inverter with a DC power supply or also as the proposed WFZ device without a DC power supply. After the device was tested in grid-connected mode in Aachen lab, field tests were performed with the Irish grid where the grid impedance was measured up to 20 kHz. The proposed impedance measurement device enables grid operators to measure impedance in real-time and additionally perform the non-parametric impedance-based stability criterion developed in RESERVE.

From the above-mentioned hardware experiments, field trials, real-time simulations etc., the requirement of network codes originally proposed have been validated and strengthened. Future converter systems require diagnostic tools such as impedance measurement, grid operators need to have devices such as WFZ device to measure grid impedance of power plants or impedance of from any node in the distribution grids. DSOs need to have real-time stability monitoring tools such as the proposed impedance driven GNC. Future converter systems need to exhibit new behaviour such as VOI control for mitigating voltage instability, analogous to LSD work for a new frequency response under low-zero inertia condition. In due course of time, with more research publications which will follow up in this area will strengthen the need for the proposed grid codes.

3. Active Voltage Management Field Trials

3.1 Background

In contrast to the requirement of the Virtual Output Impedance control technique to develop a new prototype inverter, the Active Voltage Management (AVM) Field Trials can be implemented using existing commercially available inverter technology. Electricity generation and storage technologies are experiencing significant and accelerating demand as the focus on decarbonisation and increased electrification intensifies globally. Many of these new technologies include inverters due to the fact they are coupling DC based devices to external AC networks. This presents a distinct opportunity for the AVM control technique as it can leverage inverter technology that is already being deployed for other purposes without requiring installations purely dedicated to its realisation. Indeed, many of the system stability challenges which the AVM technique has been designed to alleviate are themselves exacerbated by a proliferation of new electricity generation and storage installations. Realisation of the AVM technique should both facilitate the installation of these new technologies and allow for ever more intensive deployment on existing networks without requiring the level of investment associated with traditional electrical network capacity uprating.

In selecting specific technologies for the AVM Field Trials, it was decided to mix more established technologies such as Solar PV with more cutting-edge technologies such as Vehicle 2 Grid chargers. These selections will allow us to compare the impact of technologies on the effectiveness of the control technique across a range of network configurations located in both rural and urban environments. All AVM trial sites located in Ireland are connected to low voltage distribution networks which are operated by a single Distribution System Operator, ESB Networks. This has allowed for standardised, connection design, and monitoring and will facilitate consistent analysis of network impact.

3.2 Theory

3.2.1 Synopsis

The details of the proposed active voltage management algorithm were presented in D3.2 to D3.6. The algorithm of obtaining Volt-var Curves (VVCs) is outlined below:

- Stage 1: determines the optimal voltage across all scenarios that minimises the voltage unbalance of the feeder, or other objectives of interest, considering unlimited reactive power support for all DERs.
- Stage 2: determines the closest possible voltage deviation from optimal in each scenario, constraining the reactive power of the DER units to within representatively realistic bounds.
- Stage 3: determines the voltages that occur at varying generation levels coinciding with the voltage sensitivities of demand at these times.
- Finally, the resulting reactive power set-points (Stage 2) are plotted against the resulting voltage set-points (Stage 3) to determine the Volt-var curves for each DER system.

3.2.2 Objective Menu

In the active voltage management of low voltage distribution systems, the main objective depends on the system requirements and the availability of the controllable devices that can effectively satisfy such objectives. In such systems, the availability of the renewable energy resources and other controllable inverter-interfaced devices, enable the system operator to control the load point voltages more effectively to achieve variety range of objectives. In this project, three main objectives are considered for the active voltage management in futuristic low voltage distribution systems. These objectives are presented in Table 2.

In Table 2, the inverter types (three-/single-phase) that can help the system operator (partially) satisfy a specific objective and the network types in which a specific objective can be followed are presented. It should be noted that the effectiveness of some types of inverters are lower in satisfying some objectives and also in some types of networks. It is also possible that even with all the capacity control available in a network, the network issues cannot be fully resolved.

Code	Objective	Requirements	Three phase Network	Single phase Network
1	Voltage unbalance improvement	Single-phase inverter	✓	X
2	Loss reduction	Both Single/three-phase inverters	✓	✓
3	Improvement of voltage deviation ($V_{desired}$=1 pu.)	Both Single/three-phase inverters	✓	✓

Table 2: Objective Menu

3.2.3 Implementation of VVCs

The capacity of each inverter is limited by the maximum current that the device switches can interrupt or the thermal current limit specified by the manufacturer and by the maximum inverse bias voltage of the switches or the maximum voltage level that the device insulation can tolerate in steady state condition. In the steady state studies of power systems, these limitations are usually modelled by a single constraint, i.e., the apparent power injected by this inverter cannot be higher than the maximum allowable apparent power which is always referred to as the inverter capacity.

The reactive power support of each inverter unit should be determined considering this limitation. In fact, by measuring the voltage at the connection point of this inverter, the change in the reactive power support provided by this inverter can be found using the relevant VVC. However, it is possible that this change cannot be fully applied due to the apparent power limitation of this inverter. With P_g as Q_g as the active and reactive power injection of the inverters before developing the voltage control strategy and S^{max} as the maximum allowable apparent power of this inverter, the change in the reactive power support (ΔQ_g) should satisfy constraint **(**, where as shown in **(2)**, ΔQ_g+Q_g is the total value of the reactive power injected by this inverter.

$$-\sqrt{\left(S^{\max}\right)^2 - P_g^{\,2}} \le \Delta Q_g + Q_g \le \sqrt{\left(S^{\max}\right)^2 - P_g^{\,2}} \quad \textbf{(1)}$$

$$Q_g^{total} = \Delta Q_g + Q_g \quad \textbf{(2)}$$

Therefore, the change in the reactive power support should be found using the following steps to satisfy the inverter capacity constraints. In these steps, Q_g^{final} is the final value of the reactive power support that this inverter should provide.

1) Find the optimal change in the reactive power support of this inverter, i.e., ΔQ_g^{opt} using VVCs extracted in offline simulations.
2) If $Q_g^{total}=Q_g+\Delta Q_g^{opt}$ is between the upper and lower limits presented in (, set Q_g^{final} to Q_g^{total}.
3) If $Q_g^{total}=Q_g+\Delta Q_g^{opt}$ is greater than the upper limit (, set Q_g^{final} to the upper limit proposed by (.
4) If $Q_g^{total}=Q_g+\Delta Q_g^{opt}$ is lower than the lower limit (, set Q_g^{final} to the lower limit proposed by (.

It should be noted that other than capacity constraints, some other limitations may be applicable in the operation of special types of controllable devices. Such limitations were reviewed in **D3.3** and were applied in the case studies of that deliverable. In that case, these limitations should be

considered in the calculation of the upper and lower bounds on the reactive power support of each inverter.

3.3 Data Information Systems & Software Implementation

An initial investigation into the specific semantics from a data information systems and software implementation for each trial site carried out in D5.3 highlighted the diverse nature of interfacing with multiple DER technologies. Such diversities highlighted included communications medium, control mechanism, end device capabilities and environmental factors. In D3.6 a set of ICT architectures and requirements were defined to address some of those diversities with a view to deploying the AVM to a trial site based on the most relevant architecture. The use of these architectures in conjunction with the use of software containerisation enabled the deployment of the AVM in a structured way and in a way that allowed common software implementations and components be used across multiple trial sites. While the use of the architectures as a strong reference point simplified some elements of the deployments there were some trial site nuances that the architectures could not address. To overcome these trial site specific nuances there was a need to deploy software and hardware components to interact with inverter specific technologies and supplement communications or lack thereof to enable control and monitoring actions. The specific details of how the AVM was implemented across all trial sites is detailed in the following sections.

During the RESERVE project SERVO Live was developed as an engine of the ESB SERVO Platform that continually assesses the available capacity of the network by using near real time data from the field trial sites to calculate the network state and available capacity on the network. As detailed in Deliverable D5.1, It has been shown that SERVO Live is an efficient communications engine that can collect data from network deployed sensors or DERs connected to the network and issue instructions to these same devices. SERVO Live can display via a graphical dashboard the data it is collecting and perform calculations on the data to enable decisions to be made and broadcast to relevant network connected devices

3.4 Trial Site Implementations

3.4.1 Solar Photovoltaic (PV) Array

3.4.1.1 Background

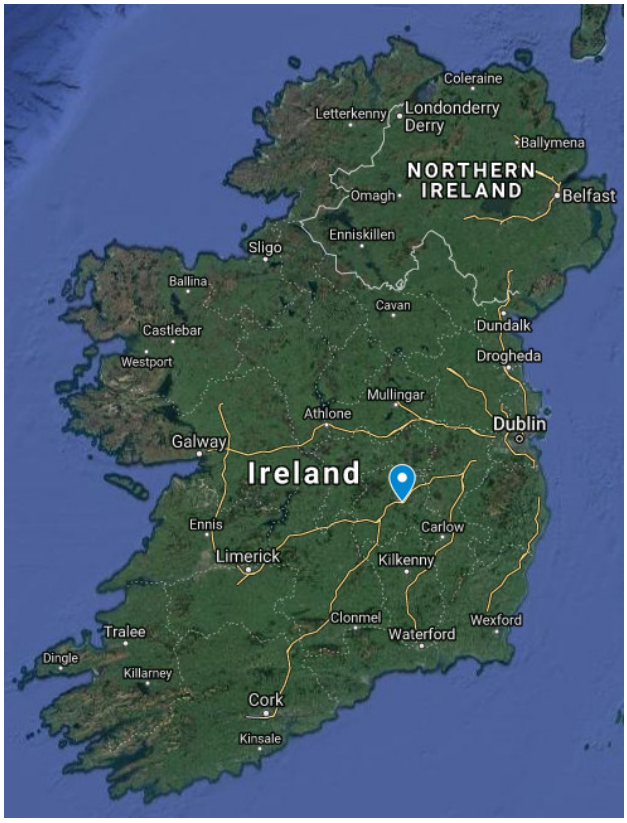

Figure 28: Location of Solar PV Array Trial Site.

Of the inverter-based technologies which are part of the RESERVE AVM Field Trials, Solar PV Arrays are possibly the most mature. There are in excess of 400 GW of Solar PV generation deployed globally which provides a very significant footprint for the realization of voltage control services. In line with this level of market maturity, techniques for communication with and the control of 'smart' inverters associated with PV installations are quite advanced. Examples include the Sunspec Alliance's Modbus interface for the control of Smart Inverters and California Energy Commission's Rule 21 governing rules for the interconnection of PV. The rate of deployment of Solar PV arrays in Ireland has lagged international norms but the recent announcement of the first national Support Scheme to specifically target Solar PV deployment is likely to yield increased levels of deployment.

3.4.1.2 Infrastructure Deployed

Figure 29: Solar PV Array in NTC, Portlaoise

The RESRVE AVM Solar PV Array Trial Site is located at ESB Network's National Training Centre in Portlaoise, Co Laois. It comprises a 7.2 kW Ground Mounted Solar PV Array connected via two independent single-phase inverters. The system was made fully operational in Q1 2018 following the completion of installation and commissioning. The relative maturity and sophistication of the inverter technology used by the PV Array was demonstrated by the fact it was possible to deploy the AVM control technique directly on the array's inverters using their standard graphical interface. This represented a marked contrast to the other technologies deployed where dedicated hardware and software had to be developed in order to realise AVM implementation.

As the Array is connected via two independent inverters it was possible to independently programme each with a standalone implementation of AVM. The additional deployment of a multi-phase Secondary Substation Sensor, see 3.4.5, allowed the project to monitor the trial's impact on the overall distribution network connected to this multi-phase connection.

3.4.1.3 Communications

The implementation of AVM on the Solar PV array from a communication perspective involved the manual configuration of the VVC points on the arrays' SMA Cluster Controller which then programmatically deploys the VVC to the inverters. Therefore, the deployment of AVM in this case did not require any communications technology, however, for an effective monitoring of the AVM performance we needed to consider some communications in order to extract the readings and inverter status for visualisation and analysis in Servo Live. Data extraction from the Solar PV Array inverters was implemented using the hardware and communications solution deployed at the V2G trial site. To fully appraise the AVM in terms of performance and overall effect on the Solar PV array it was necessary to access a high granularity of reading and to ensure this, a bespoke Raspberry Pi and Cradle Point was required to access the readings from the inverter and communicate those readings to Servo Live.

3.4.1.4 Data Information Systems & Software

As stated in Section 3.4.2.3 the only communications required for the Solar PV array was centred around the monitoring of the device and in particular the performance of the AVM. The initial investigation of how we would extract the readings from the device lead us to believe that the inverter manufacturers, SMA, provided visualisation and API access to the readings.

However, the level of granularity required to validate and assess the performance of the AVM was not high enough via the SMA API and to access a higher granularity would require a vendor subscription to a proprietary API. To overcome this, access to the Modbus streams for each inverter was required. This provided access to the high granularity of readings for each inverter and was achieved by connecting a Raspberry Pi to the cluster controller via an ethernet port which utilised a Python script to parse the relevant Modbus registries and transfer the data to Servo Live via MQTT.

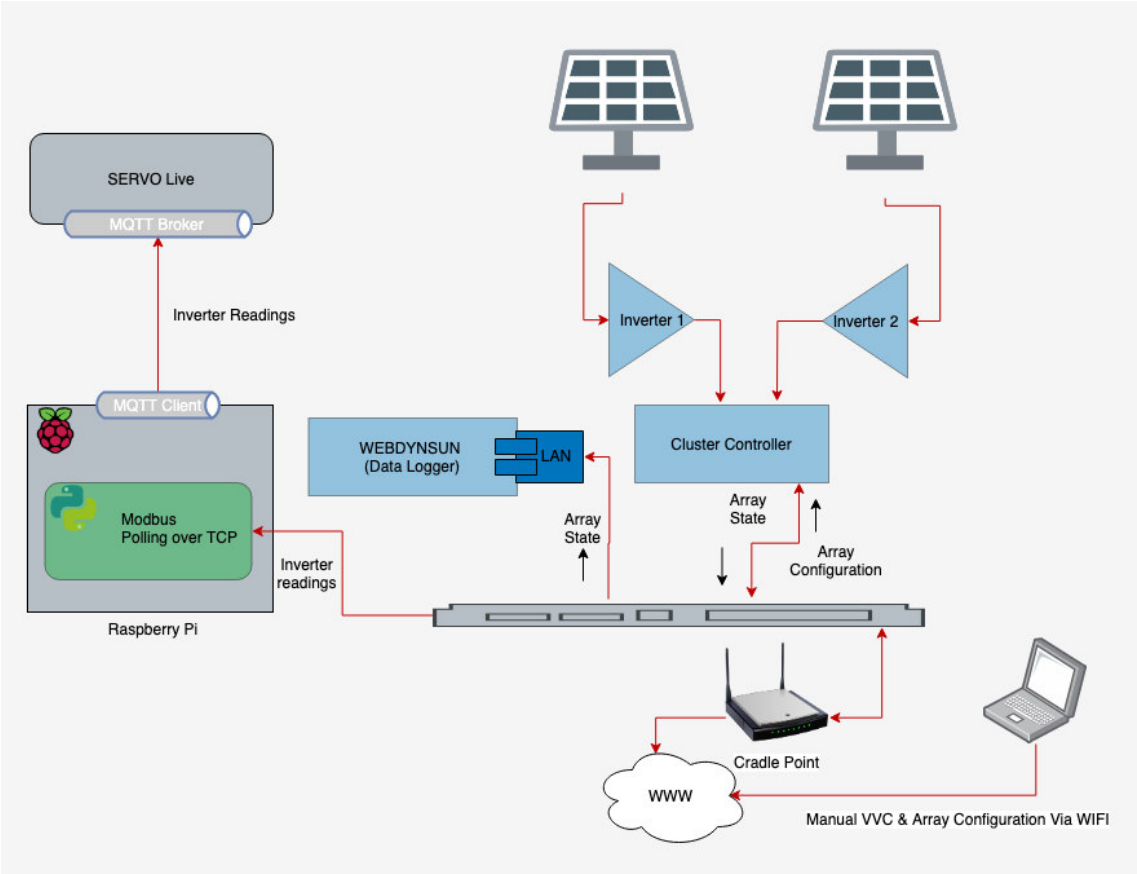

Figure 30: Communications Architecture of Solar PV Array Trial Site

3.4.1.5 Tuning of AVM Algorithm to Specific Site

Figure 31 shows the single-line diagram of a small low voltage distribution system connected to the upstream system at the local secondary substation. Additional DERs including two PV arrays and a wind turbine are connected to this system at different connection points. Only the new PV array has a controllable inverter, and the other DERs are assumed to work at a fixed power factor (0.95 lagging). Due to the lack of absolute data, some assumptions have been made. In

Figure 31, these assumptions are distinguished in red.

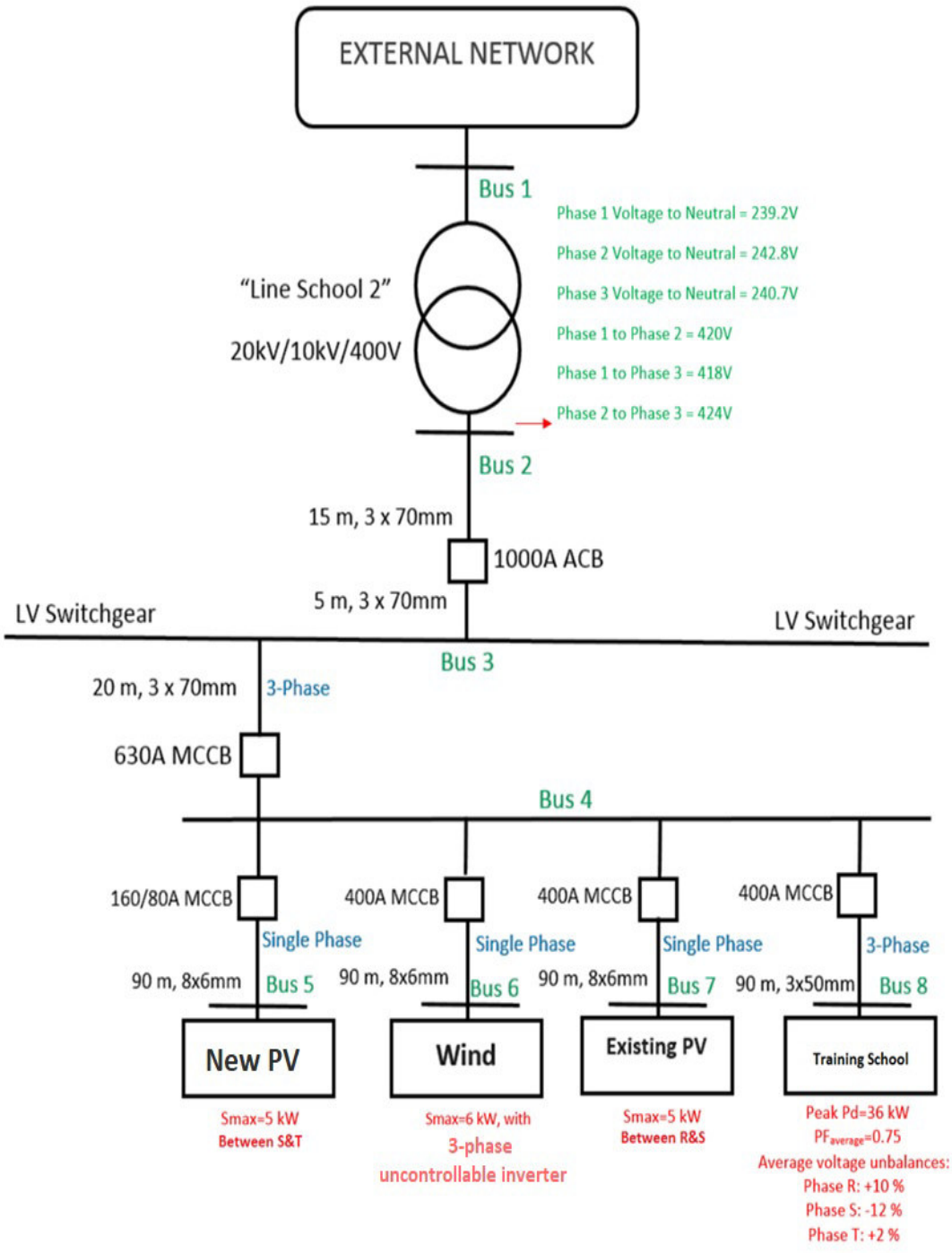

Figure 31 Single-line diagram of the small feeder at Portlaoise (trial site RES-PV-NTC-0) for DER installation.

Scenario	Load Factor	Z	I (P=1-Z-I)	Power Factor	Un_a (%)	Un_b (%)	Un_c (%)	$P_{existing}/S_{existing}$	P_{wind}/S_{wind}	P_{new}/S_{new}
1	0.7	0.4	0.2	0.9	10.36	-10.4	2.95	0	0	0
2	0.6	0.4	0.2	0.85	10.3	-9.6	2.19	0	0.25	0
3	0.5	0.2	0.3	0.86	11.48	-9.67	1.03	0	0.5	0
4	0.5	0.2	0.3	0.87	9.25	-9.92	1.75	0	0.75	0
5	0.5	0.3	0.25	0.87	9.4	-9.6	0.32	0	0.75	0
6	0.6	0.3	0.2	0.85	9.52	-9.67	2.72	0	0.5	0
7	0.6	0.4	0.2	0.86	10.17	-10.64	2.64	0	0.5	0
8	0.7	0.4	0.2	0.87	11.49	-10.74	2.45	0.25	1	0.5
9	0.8	0.4	0.2	0.86	11.41	-9	0.78	0.5	0.75	0.5
10	0.75	0.3	0.25	0.88	9.18	-10.66	1.78	0.25	0.5	0.5
11	0.8	0.5	0.1	0.86	10.2	-10.93	0.07	0.5	0.25	0.75
12	0.8	0.4	0.1	0.87	10.58	-9.88	1.28	0.5	0	0.5
13	0.8	0.4	0.2	0.88	10.25	-9.24	0.94	0.5	0.25	0.75
14	0.8	0.4	0.2	0.89	10.97	-9.66	0.48	1	0.25	1
15	0.8	0.5	0.15	0.9	10.88	-10.62	0.54	0.75	0.25	0.75
16	0.8	0.55	0.25	0.9	9.88	-10.26	1.27	1	0.25	0.75
17	0.8	0.4	0.2	0.91	10.29	-10.08	0.28	0.75	0.5	0.75
18	0.85	0.4	0.2	0.93	9.05	-9.04	1.8	1	0.5	1
19	0.9	0.45	0.2	0.91	11.95	-10.69	1.41	1	0.25	1
20	0.85	0.4	0.2	0.93	9.5	-9.29	2.09	0.75	0	0.5
21	0.88	0.45	0.2	0.94	9.32	-9.71	2.1	0.75	0.25	0.75
22	0.9	0.4	0.2	0.92	10.12	-10.25	1.92	0.5	0.5	0.5
23	0.9	0.45	0.2	0.93	9.59	-10.62	0.1	0.5	0.5	0.5
24	0.85	0.4	0.2	0.95	10.47	-10.14	0.21	0.5	0.5	0.75
25	0.85	0.4	0.1	0.93	10.02	-10.04	0.96	0.75	0.5	0.75
26	0.9	0.5	0.15	0.93	11.85	-10.76	1.59	0.25	0.75	0.5
27	0.95	0.5	0.2	0.94	11.76	-9.82	1.96	0.25	0.5	0.25
28	1	0.6	0.1	0.93	9.16	-10.55	1.22	0	0.75	0
29	1	0.65	0.1	0.93	11.21	-10.23	2.46	0	0.75	0

30	0.9	0.7	0.1	0.96	9.81	-9.83	2.16	0	0.5	0
31	0.9	0.6	0.2	0.95	10.27	-10.5	2.91	0	1	0
32	0.95	0.75	0.05	0.95	10.64	-10.42	1.59	0	0.75	0
33	0.8	0.6	0.2	0.94	11.83	-9.77	0.98	0	0.5	0
34	0.8	0.75	0.05	0.93	10.25	-10.47	0.32	0	0.25	0
35	0.75	0.6	0.2	0.92	11.95	-9.35	1.83	0	0	0

Table 3 Trial site Solar PV NTC

Table 3 gives the operation scenarios. In this table, P_{new}, P_{wind}, and $P_{existing}$ are the power injected by the new photovoltaic array, wind turbine and existing photovoltaic. Coefficients of the ZIP load model are given by Z, I and P, for constant impedance, constant current and constant power components, respectively.

Load Factor (LF) determines the ratio of the active power consumption and the maximum power consumption presented in Table 3. Power Factor (PF) is also presented in Table 3. This table also shows the load unbalance distribution on phases (R), (S) and (T) at the load point. Finally, Table 4 shows how to calculate the active and reactive power demands on phase (a). The active and reactive power consumptions on two other phases are found similarly.

$$P_{a,s} = P_a^{max}.\mathrm{LF}_s.(1+\mathrm{Un}_{a,s}/100)$$
$$Q_{a,s} = P_{a,s}.\mathrm{PF}_s$$

Equation 2

Phase a		Phase b		Phase c	
Pmax (kW)	**Qmax (kvar)**	**Pmax (kW)**	**Qmax (kvar)**	**Pmax(kW)**	**Qmax (kvar)**
12	8	12	8	12	8

Table 4 Maximum Load on each phase at bus 8

3.4.1.5.1 VVCs of the network RESs for minimisation of the voltage unbalance

The only controllable DER in this simple system is the new solar array installed at bus 5 between phases S and T. Other two RESs (existing PV array and wind turbine) are not controllable. In this subsection the first objective function (Table 2) is considered in order to apply the proposed active voltage management algorithm and extract the VVC for this trial site. The VVC is presented in Figure 32 for the new PV array. The slope and intercept of the VVC are given by m and c, respectively.

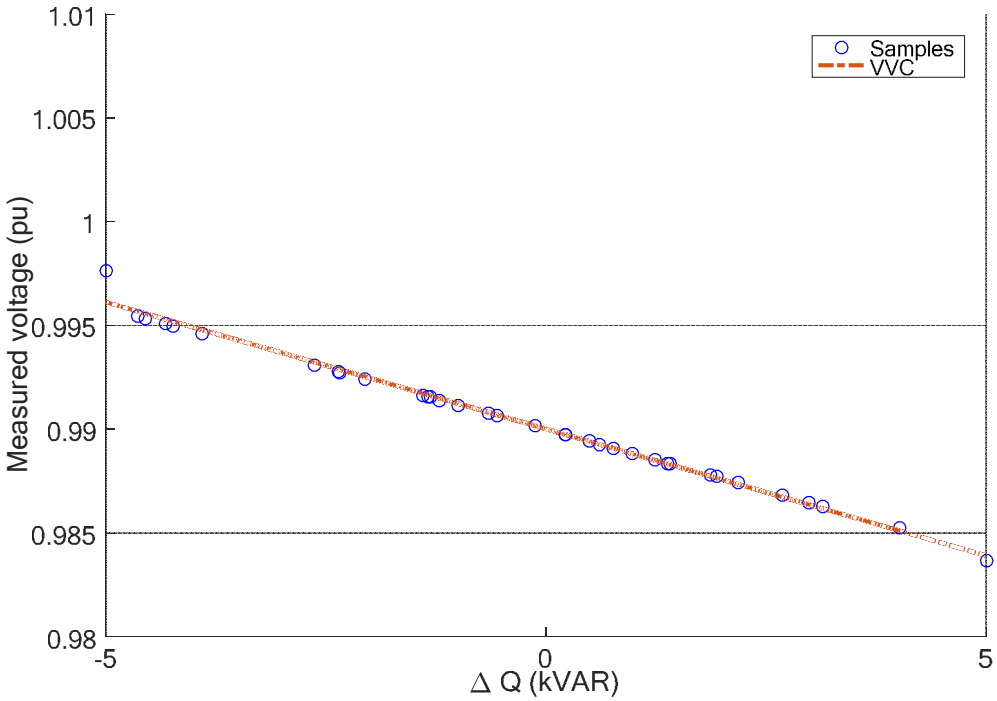

Figure 32 VVC of existing PV for voltage unbalance minimisation (m= -0.00122 (pu/kvar), c= 0.99002 pu).

3.4.1.5.2 VVCs of the network RESs for minimisation of total loss

The second objective is considered here to apply the active voltage management algorithm. The final VVC for the new PV array as the only controllable device is presented in Figure 33**.**

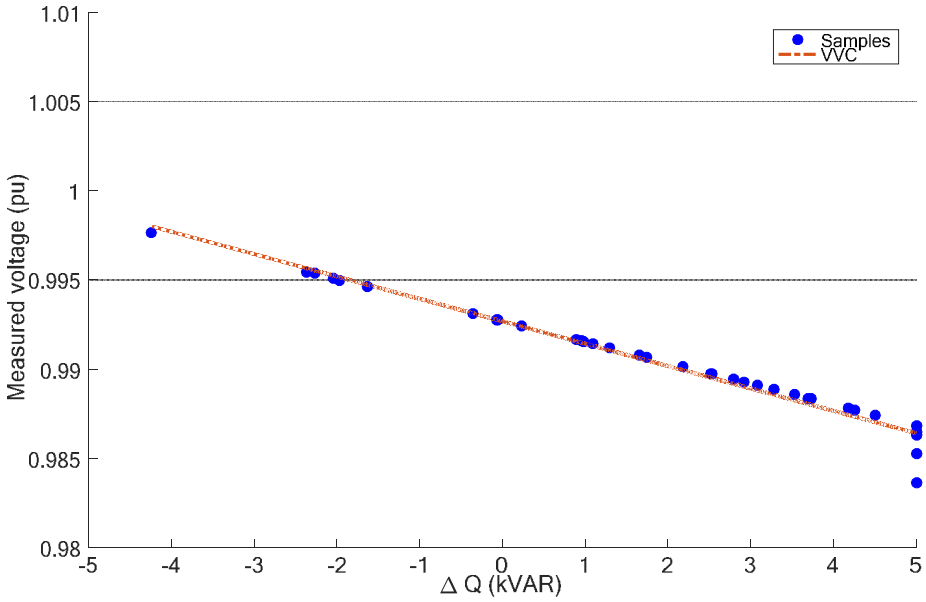

Figure 33 VVC of the new PV array for loss minimisation (m= -0.001254 (pu/kvar), c= 0.99268 (pu)).

3.4.1.5.3 VVCs of the network RESs for minimisation of the voltage deviation from $V_{desired}$=1 pu at load point (bus 8)

The third objective function is considered here for extracting the VVCs using the proposed active voltage management algorithm in this trial sites. In this case, the active voltage management algorithm suggests that all the inverters should inject their maximum reactive capacity.

It should be noted that in every possible scenario, the active power production of each DER is determined by the availability of the relevant source. For instance, the solar radiation determines the active power production of the system PV arrays. With the objective considered in this subsection, the inverters should fully dedicate their remaining capacities to provide positive reactive power support. As an example, if the active production of the new PV is 2 kW then this DER should inject 3 kvar reactive power (capacity of this DER is 5 kVA).

3.4.1.5.4 Summary of VVCs for this trial site

Objective	**Reactive power control mode**		**Voltage control mode**
	m (pu/kvar)	**c (pu)**	**V_{opt}**
Voltage Unbalance	-0.001221	0.99002	0.99005
Energy Loss	-0.001254	0.99268	0.99267
Voltage Deviation	NA	NA	1.01031

Table 5 VVC for the new PV array in both modes of operation

Finally, it should be noted that if the VVC proposes a reactive power support beyond the inverters' upper or lower limits, the reactive power support is set to the adjacent limit. Table 5 summarises the VVCs for this trial site. It should be noted that these VVCs are extracted with this assumption that all the inverters are operated under the reactive power control mode of operation. For voltage control mode, a voltage is proposed for each converter and of course for each objective. Table 5 also gives these voltages.

3.4.1.6 Performance of AVM Algorithm

In order to analyse the performance of the AVM algorithm for the Solar PV Array trial site it was necessary to extract data measurands from both the Solar PV inverters and the relevant secondary substation sensor. The deployment of secondary substation sensors for a period before the AVM control technique was implemented allowed the recording of baseline network performance in the absence of AVM implementation. SERVO Live provided a straightforward interface for the extraction of these correlated datasets for external analysis. Figure 34 illustrates such measured data from this trial site including: voltage, active and reactive power, as displayed in the SERVO Live dashboard.

Figure 34: Measured data monitoring dashboard for solar photovoltaic array trial site.

The assessment of the impact of the AVM algorithm necessitated the comparison of network performance in two scenarios, namely with and without the AVM control technique algorithm in operation. This comparison of electrical power imported from the upstream secondary substation is plotted in Figure 35, for both scenarios. Offline technical analysis of these data plots calculated that the introduction of the AVM algorithm effectively reduced the active power consumption at the point of connection by 4.92%. This reduction in energy loss is attributable to reductions in active power losses due to the optimisation of reactive power injections by the inverters.

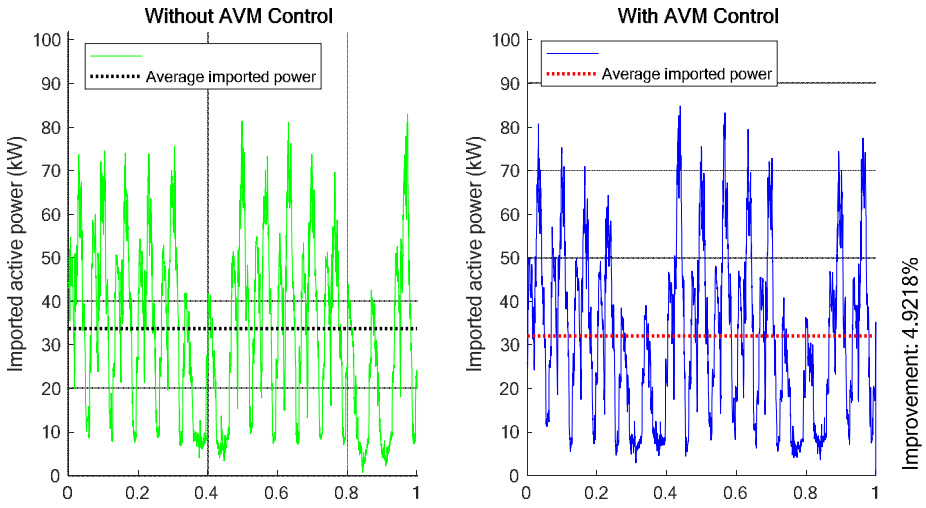

Figure 35: Performance evaluation of AVM algorithm for Solar Photovoltaic Array.

3.4.2 Vehicle to Grid (V2G) Charger

3.4.2.1 Background

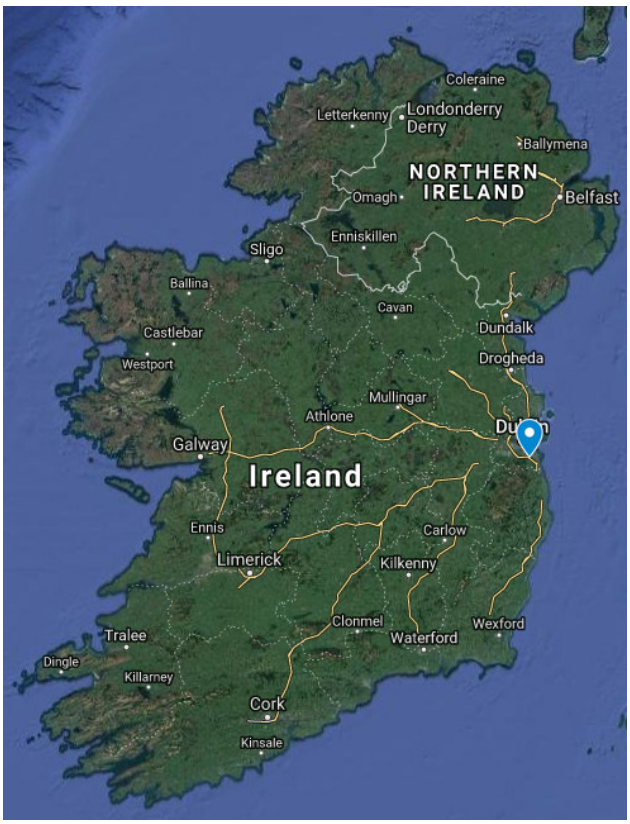

Figure 36: Location of V2G Charger Trial Site.

A central pillar of Ireland's and the EU's decarbonisation strategy is the electrification of the transport fleet. In the first instance this drives a requirement for vehicle charging infrastructure and a consequent significant increase in electricity demand. A viable further consequence of this transformation is the potential for the electricity network to leverage electric vehicle batteries when they are connected to the system via charging infrastructure. Technologies that can provide bi-directional (i.e. both charge an electric vehicle and extract charge for injection back into the grid) are known as Vehicle to Grid (V2G) chargers. As V2G chargers require the capability to convert DC power, extracted from the vehicle battery, into AC power for injection into the distribution network, controllable inverters are an essential component of the technology. Unit costs for V2G charger devices have fallen rapidly in line with increasing levels of EV deployment and there is an expectation that V2G functionality will be built directly into vehicles if monetization of available system services is achieved.

3.4.2.2 Infrastructure Deployed

Figure 37: V2G Charger Infrastructure

The RESERVE Field Trial V2G Charger installation is located at ESB Networks offices in Leopardstown, Dublin. It is the first V2G installation located in Ireland. The device itself is rated at 10 kVA for both charging and discharging and connects to EVs over the CHAdeMO charging protocol. The installation was designed with a large interface kiosk (which can be seen on the left of the above image) which has allowed for collaborative use of the device with the Horizon 2020 SUCCESS project. The Field trial location sees throughput of EVs during the working week (Monday – Friday) but vehicles are never present at evenings or weekends. Given this could limit the scale and scope of testing for the RESERVE project a Nissan Leaf EV has been procured in order to provide continued dedicated access to a battery. Installation of the V2G Charger and associated infrastructure was completed in Q2 2018.

In line with the technologies deployed across the other field trials in Ireland the V2G system leverages the capabilities of its on-board inverter in order to implement voltage control techniques. However, the relative immaturity of the market for V2G systems was evidenced by the lack of sophistication of the V2G device which necessitated the deployment of additional hardware by the project team so that it could interface with our monitoring platform. This lack of technological maturity and robustness was further evidenced by the fact that the original V2G hardware configuration was not capable of implementing the dynamic reactive power support which it was specified to provide. Following extensive engagement with the Original Equipment Manufacturer (OEM) it was determined that no previous customer had attempted to implement such functionality on this model of device so it's failure to match its stated specification had not been previously identified. Further engagement and design development work with OEM allowed both hardware and software upgrades to the V2G charger's internal components to be completed and thus facilitate successful implementation of reactive power injection into the local distribution network.

3.4.2.3 Communications

There were two perspectives for which communications technologies had to be deployed for the V2G installation. The first was to facilitate the deployment of the AVM technique and the second was in the sending of monitoring data from the V2G to SERVO Live for processing. To achieve

this, it was necessary to develop a schema that would facilitate communications from both inside and outside the V2Gs' Local Area Network (LAN). Given that the V2G Charge Point and its inverter only has a proprietary API it did not have the relevant communications interface for the AVM integration and so it was necessary to deploy an edge computing device (Raspberry Pi) onsite. The Raspberry Pi is connected to the Charge Point via ethernet to communicate with the device and to the central AVM controller via a mobile network hotspot. To facilitate communication both the central controller and SERVO Live monitoring component have an authenticated MQTT broker as a medium to transport TLSv1.2 encrypted payloads to and from the Raspberry Pi.

3.4.2.4 Data Information Systems & Software

The implementation of the AVM, in this case, is centred on the decentralised ICT architecture (as described in WP3 deliverable D3.6) and relies on minimal communication between the central controller in terms of VVC execution. This means that the VVC is sent to the edge for implementation either on an edge computing device, as is the case here, or on the actual inverter. To decide where the VVC must be executed in the V2G charger installation it must be noted that the V2G inverter does not have the capabilities to accept a VVC and execute it, therefore it was necessary to deploy a software component to execute the VVC on the edge device Raspberry Pi. While the communications between the Raspberry Pi and the V2G inverter is carried out over ethernet in software terms, the interface used to access the control mechanisms and data access functionality on the inverter is a Python program developed by V2G OEM and to access this a client library provided by the OEM was required to be installed on the Raspberry Pi. This enabled the RESERVE development team to integrate the readings taken from the inverter and use them in the execution of the VVC. It also allowed for the delivery of the generated power factor set point value to the V2G inverter, which maintained a stable voltage on the V2G. While the readings are used to execute the VVC they are also forwarded to SERVO Live via MQTT to be visualised on a dashboard for analysis and verification.

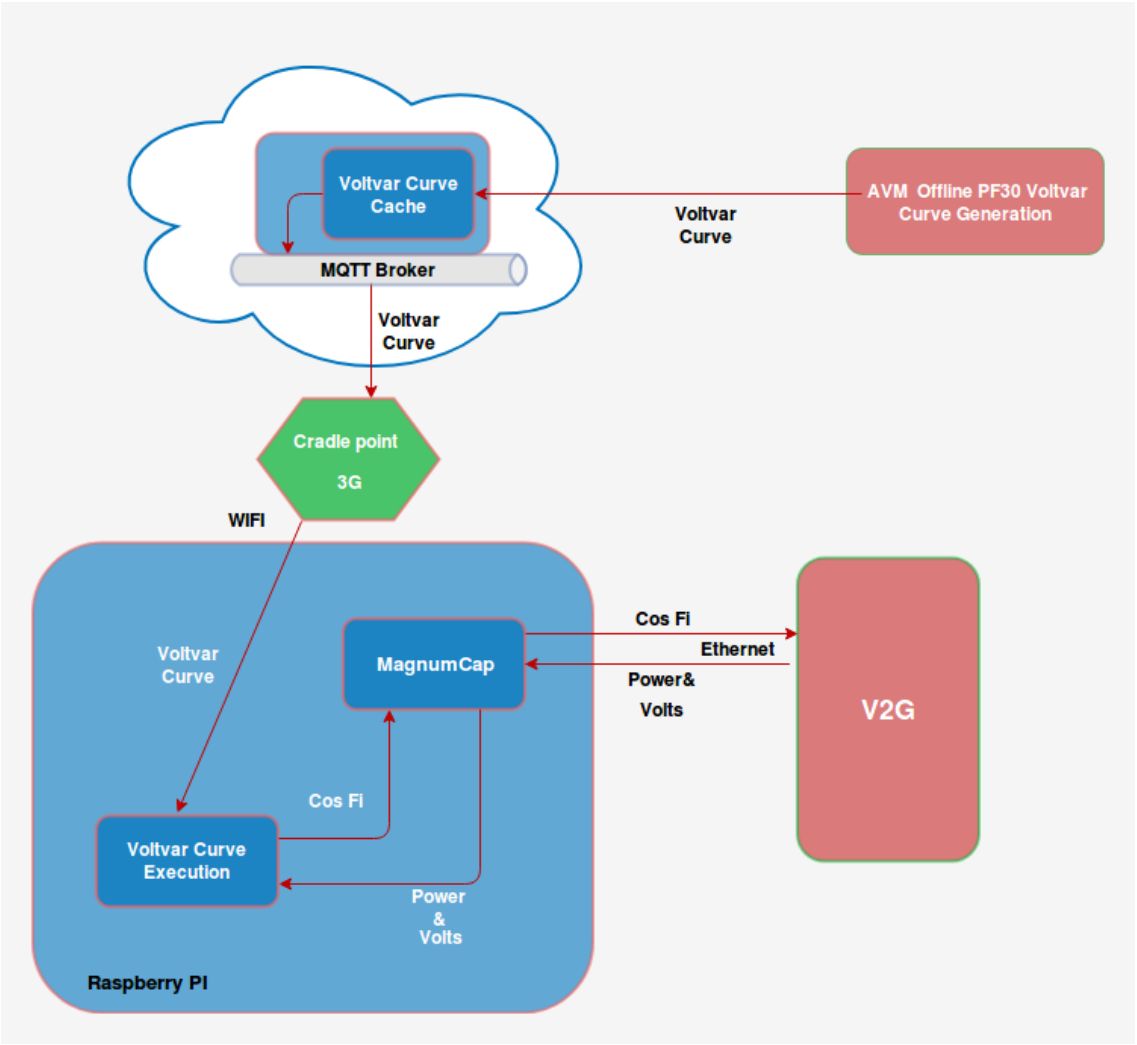

Figure 38: Communications Architecture of V2G Trial Site

3.4.2.5 Tuning of AVM Algorithm to Specific Site

3.4.2.5.1 Input data and assumptions for V2G test site

Figure 39 shows the single-line diagram of a small feeder connected to the upstream system at Leopardstown for V2G charger installation. The batteries of the electric vehicles are connected using a three-phase inverter at the V2G charge point. The battery power injection capacity is assumed to be 3 kW for each electric vehicle other than that connected to the higher capacity V2G charger. The inverter capacity is considered to be 9 kVA. This inverter is a three-phase inverter. Therefore, minimisation of the voltage unbalance cannot be considered here as an objective.

It should be noted that V2G systems typically consume active power, except for the systems for which both operation strategies and technical characteristics of the charging station allow battery discharge. The owners of the electric vehicles may also raise an argument about discharging their vehicles' batteries in the course of time that they left their vehicles to be charged. In other words, the interface between the distribution grid and the EVs, instead of using typical power converters that only work on unidirectional mode, needs to use bidirectional power converters to charge the batteries (G2V - Grid-to-Vehicle mode) and to deliver part of the stored energy in the batteries back to the power grid (V2G - Vehicle-to-Grid mode). Usage profiles should be defined and controlled by a collaborative broker, considering the requirements of the low voltage distribution systems and the conveniences of the vehicle owners. In this section, it has been assumed that the charging station only consumes active

power. However, reactive power can be easily exchanged between the V2G system and the grid.

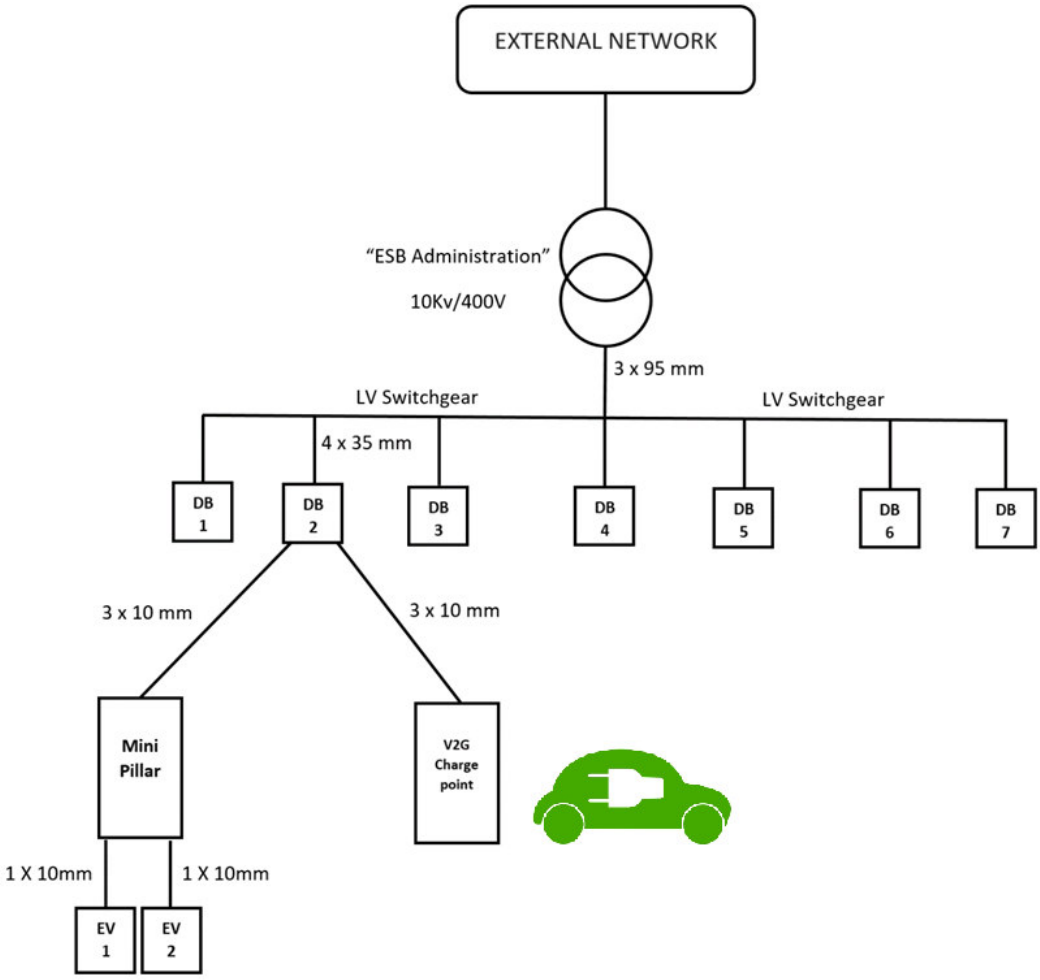

Figure 39 Single-line diagram of the small feeder at Leopardstown (trial site RES-V2G-LEOP-0) for V2G charger installation.

Table 6 gives the scenarios. In this table, P_{V2G} is the power injected to the system at PCC by the V2G charger. Coefficients of the ZIP load model are given by Z, I and P, for constant impedance, constant current and constant power components, respectively. Power Factor (PF) at the system load points is presented in Table 6 for different scenarios. The load has an unbalanced distribution on phases (a), (b) and (c) at all load points (DB 1 to DB 7). Table 7 shows how to calculate the active and reactive power demands on phase (a). The active and reactive power consumptions on other phases can be found similarly.

Scenario	Load Factor	P_{V2G} /S_{V2G}	Z	I	Power Factor	Un_a (%)	Un_b (%)	Un_c (%)
1	0.7	-0.1429	0.400	0.200	0.900	10.36	-10.4	2.95
2	0.6	0.0000	0.400	0.200	0.850	-10.3	9.6	2.19
3	0.5	0.0000	0.200	0.300	0.860	11.48	-9.67	1.03
4	0.5	-0.2857	0.200	0.300	0.870	9.25	-9.92	1.75
5	0.5	0.0000	0.300	0.250	0.870	-9.4	9.6	0.32
6	0.6	-0.4286	0.300	0.200	0.850	9.52	-9.67	2.72
7	0.6	0.0000	0.400	0.200	0.860	-10.17	10.64	2.64
8	0.7	-0.1429	0.400	0.200	0.870	11.49	-10.74	2.45
9	0.8	-0.2857	0.400	0.200	0.860	-11.41	9	0.78
10	0.75	-0.2857	0.300	0.250	0.880	9.18	-10.66	1.78
11	0.8	-0.2857	0.500	0.100	0.860	10.2	-10.93	0.07
12	0.8	0.0000	0.400	0.100	0.870	-10.58	9.88	1.28
13	0.8	-0.4286	0.400	0.200	0.880	10.25	-9.24	0.94
14	0.8	-0.5714	0.400	0.200	0.890	10.97	-9.66	0.48
15	0.8	-0.4286	0.500	0.150	0.900	-10.88	10.62	0.54
16	0.8	-0.5714	0.550	0.250	0.900	9.88	-10.26	1.27
17	0.8	-0.4286	0.400	0.200	0.910	-10.29	10.08	0.28
18	0.85	-0.5714	0.400	0.200	0.930	9.05	-9.04	1.8
19	0.9	-0.5714	0.450	0.200	0.910	-11.95	10.69	1.41
20	0.85	-0.4286	0.400	0.200	0.930	9.5	-9.29	2.09
21	0.88	-0.4286	0.450	0.200	0.940	-9.32	9.71	2.1
22	0.9	0.0000	0.400	0.200	0.920	10.12	-10.25	1.92
23	0.9	-0.2857	0.450	0.200	0.930	-9.59	10.62	0.1

24	0.85	-0.2857	0.400	0.200	0.950	-10.47	10.14	0.21
25	0.85	0.0000	0.400	0.100	0.930	10.02	-10.04	0.96
26	0.9	-0.1429	0.500	0.150	0.930	-11.85	10.76	1.59
27	0.95	-0.4286	0.500	0.200	0.940	11.76	-9.82	1.96
28	1	0.0000	0.600	0.100	0.930	-9.16	10.55	1.22
29	1	-0.2857	0.650	0.100	0.930	11.21	-10.23	2.46
30	0.9	-0.2857	0.700	0.100	0.960	-9.81	9.83	2.16
31	0.9	-0.1429	0.600	0.200	0.950	10.27	-10.5	2.91
32	0.95	0.0000	0.750	0.050	0.950	-10.64	10.42	1.59
33	0.8	-0.2857	0.600	0.200	0.940	11.83	-9.77	0.98
34	0.8	0.0000	0.750	0.050	0.930	-10.25	10.47	0.32
35	0.75	-0.2857	0.600	0.200	0.920	11.95	-9.35	1.83

Table 6 Scenarios for V2G Leopardstown

Phase a		Phase b		Phase c	
P^{max} (kW)	Q^{max} (kvar)	P^{max} (kW)	Q^{max} (kvar)	P^{max}(kW)	Q^{max} (kvar)
2.2	0.75	2.2	0.75	2.2	0.75

Table 7 Maximum Load on each phase at each load point (DB 1 to DB 7)

3.4.2.5.2 VVCs of the network RESs for minimisation of the voltage unbalance

With a three-phase inverter, the voltage unbalance cannot be effectively improved in distribution systems. This is due to the fact that each phase of the three-phase controllable devices cannot be controlled separately, and a single control unit provides the gate pulses for the inverter switches. Therefore, this inverter cannot be used to optimise the voltage unbalance in this network.

3.4.2.5.3 VVCs of the network RESs for minimisation of the total loss

The only controllable DER in this simple system is a three-phase V2G system. In this subsection the second objective function is considered in order to apply the proposed active voltage management algorithm and extract the VVC in this trial site. The final VVC for the V2G system as the only controllable device is presented in Figure 40.

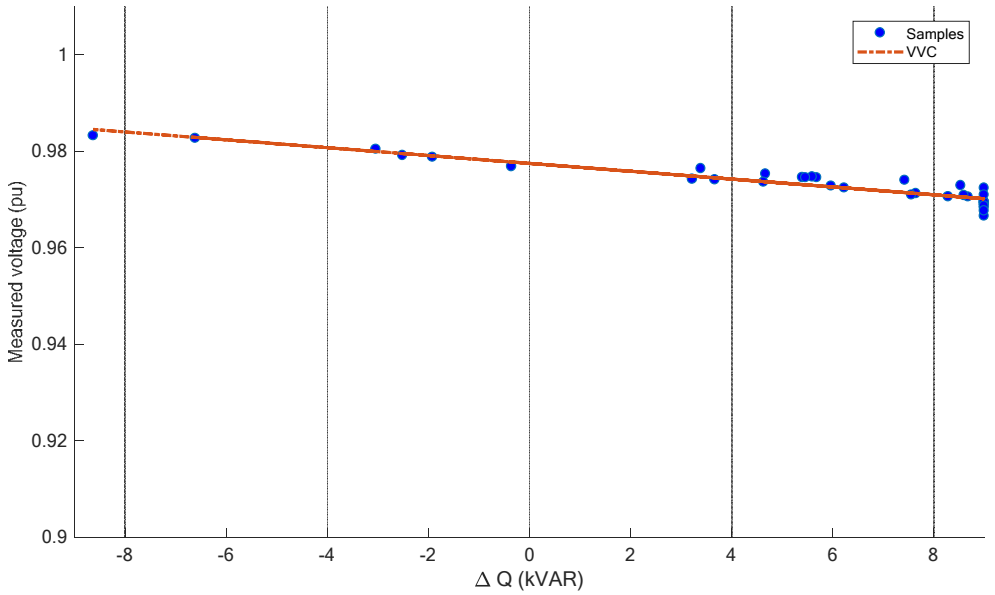

Figure 40 VVC of the new V2G for loss minimisation (m= -0.0008132 (pu/kvar), c= 0.977487 (pu), V_{opt}=0.977445 (pu)).

3.4.2.5.4 VVCs of the network RESs for minimisation of the voltage deviation from $V_{desired}$=1 pu at load points (DB 1 to DB 7)

Considering the third objective function for extracting the VVCs using the proposed active voltage management algorithm in this trial site, the AVM algorithm suggests that this inverter should inject its maximum reactive capacity in all possible scenarios. Therefore, no VVC can be found for this system with this objective. It should be noted that in every possible scenario, the active power production of each DER is determined by the availability of the regarding source, e.g., solar radiation and wind.

3.4.2.5.5 Summary of VVCs for this trial site

As discussed before, if the VVC proposes a reactive power support beyond the inverters' upper or lower limits, the reactive power support is set to the adjacent limit.

Table 8 summarizes the VVCs for this trial site. It should be noted that these VVCs are extracted assuming all the inverters working under power control mode of operation. For voltage control mode of operation, a voltage is proposed for each converter and of course for each objective. Table 8 also presents such voltage levels.

	Reactive power control mode		**Voltage control mode**
	m (pu/kvar)	**c (pu)**	**V_{opt}**
Voltage Unbalance	NA	NA	NA
Energy Loss	-0.0008132	0.977487	0.977445
Voltage Deviation	NA	NA	1.00372

Table 8: VVC for the V2G system in both modes of operation for RES-V2G-LEOP-0

3.4.2.6 Performance of AVM Algorithm

The AVM Voltage control technique produced a VVC optimised for the characteristics of the V2G trial site as detailed in section 3.4.2.5. When implementing this deployment in the field the communications infrastructure described in section 3.4.2.4 proved capable of extracting system performance measurands from the V2G device, executing the AVM calculations locally on this hardware and communicating relevant measurands and set-point to both the V2G device and the Servo Live monitoring platform. Challenges emerged with regard to the actual implementation of the AVM technique determined Power Factor set-points by the V2G device itself. A detailed re-evaluation of the tuned VVCs calculated for the trial site was undertaken and is included in Appendix A.

Extensive analysis and debugging identified the failure to accurately track Power Factor set-points as being due to the performance of the V2G device itself. The discovery of this fact led to extensive engagements with the V2G OEM in order to identify and develop a solution for this issue as discussed in section 3.4.2.2. These engagements led to the design of a re-engineered communication and control module for the V2G unit which incorporated extensive additional software features developed by the OEM. Initial testing demonstrated that the re-engineered modules were capable of providing a level of reactive power support when requested with a consequent impact on network voltage, see Figure 41.

Figure 41: V2G Device undergoing Charge/Discharge cycles with resultant impact on reactive power delivered and system voltage.

Further testing revealed however that level of precision of the revised OEM device implementation was not of sufficient accuracy to allow for the precise tracking of set-points as required by the AVM technique. This lack of precision can be viewed in where an approximate 6% differential between the specified and measured V2G device Power Factor is evident.

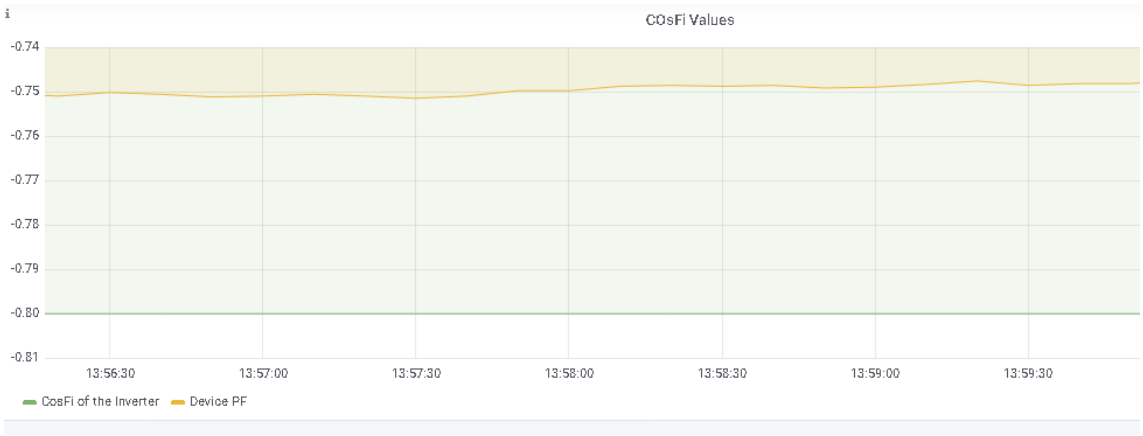

Figure 42: Power Factor Setpoint (CosFi of the Inverter) vs Measured Power Factor (Device PF) of the V2G Inverter

These learnings served to highlight that despite the accurate development of a bespoke AVM solution for this particular trial site, based on the specified capabilities of the V2G device as procured, that the differential between expected device performance and actual outturn capability did not align. This appears to be a particular issue in relation to emerging technologies such as V2G which do not have the established scale of deployment or technological maturity of the other DERs technologies deployed in these trials.

3.4.3 Domestic Scale Battery Storage Sites

3.4.3.1 Background

Figure 43: Location of Domestic Scale Battery Trial Sites.

Since electricity networks require instantaneous demand to be met by instantaneous generation, the rise of intermittent renewable generation poses a complex problem for system balancing. One potential solution to the variance of renewable generation is the utilisation of energy storage. Large-scale storage facilities have been in existence for many decades using technologies such as pumped-storage hydroelectricity. The recent collapse in the unit cost of Lithium-ion batteries has resulted in small-scale domestic scale storage installations becoming increasingly commercially viable. As such systems require an inverter to convert from DC to AC, they are another viable technology for the deployment of the AVM control technique. Domestic scale battery systems also provide for additional use cases including; price arbitrage due to their ability to store electricity imported from the distribution network, allowing the installation of increased levels of small-scale generation without the need to spill excess generation into the network and additional opportunities to provide system services.

3.4.3.2 Infrastructure Deployed

Figure 44: Battery Storage System installed at Nenagh Library

A total of three sites were included as Domestic Scale Battery Storage sites for Field Trials of the AVM control technique within RESERVE. The sites comprised a mixture of domestic, and institutional premises located in both urban and rural settings. Two of the sites coupled the battery systems with local small-scale generation. Li-Ion batteries with a capacity of 10 - 12 kVA manufactured by a range of OEMs were installed at each of the locations. The first 'live' Battery Storage site located at Killumney in Co. Cork commenced operation in Q3 2018.

A unique feature of the domestic scale battery trial sites is the fact that the technology was not directly deployed by the project itself but instead developed in partnership with a commercial aggregator. The aggregator identified suitable customers and locations for the battery deployments in order to assess the commercial viability of the technology in the Irish market. Through engagement with this aggregator the project was able to rapidly increase the pool of potential trial sites in return for a relatively small increase in deployment costs. The costs associated with the batteries themselves, installation works and integration into communication networks was met by the aggregator as per their business model. The RESERVE project was then able to leverage this investment through the implementation of the AVM control technique across this same infrastructure. In effect the AVM deployment operated in parallel with the batteries' commercial operation providing additional network benefits from a single installation. This model of implementation offers a very attractive and cost-effective model for the efficient mass deployment of the AVM control technique far beyond what is viable through the roll-out of dedicated devices. The model of voltage control provision through aggregators does present specific challenges however as the commitment of any specific site to engage in the provision of services is not absolute. This was evidenced in the course of the project trials where a number of battery installations initially identified for inclusion in the suite of trial sites could not be progressed due to changes of building ownership, customer concerns regarding impacts on device performance or longevity and the expiration of commercial agreements with the aggregator. Such challenges highlight the need for robust processes and commercial agreements in order to ensure the continuity of service provision in any larger scale deployment.

3.4.3.3 Communications

The architecture of these sites was modelled on the Centralised System detailed in the D3.6 report which means that the execution of the Volt-var Curve (VVC) had to be carried out in a central location away from the inverter on site. The reason for choosing this centralised approach was due to the inverters being behind an aggregator platform. The RESERVE development team had to integrate and communicate with that aggregator platform directly. This factor drove the communication requirements for this integration in terms of the technology used

to transfer the data and the protocol used for both entities to communicate with. This communication is carried out over an SSL secured and encrypted MQTT broker to broker channel for both the receipt of the readings and the sending of the Reactive Power set-points back to the DER Unit. In tandem with the monitoring of the performance of the AVM at the inverter level it is also important to provide monitoring at a network level to assess the impact of the AVM on the network. This was achieved with the use of a pole mounted LV sensor installed at the secondary substation with the measured data transmitted to SERVO Live for visualisation and analysis via MQTT.

3.4.3.4 Data Information Systems & Software

The diagram in Figure 45 demonstrates the components and data flow for the execution of the AVM technique on the Battery Trial Site(s). In this case the central cloud server contains components that are responsible for the receipt of the VVC from the AVM Offline 3 Phase-OPF application, the storage, the storage of that VVC, the receipt of the readings, the execution of the VVC and the subsequent sending of the set-point back to the trial site. Each component within the cloud server is built in a modular way and uses Docker as a containerisation tool to host the running software.

The VVC objects are stored within a database hosted on the cloud server that only the AVM can access. The AVM itself is run within a Docker container on a Linux Server. The MQTT broker that both the trial site and AVM use to communicate is also hosted in the central cloud server. The communication between site and server is encrypted to ensure the messages are trustworthy.

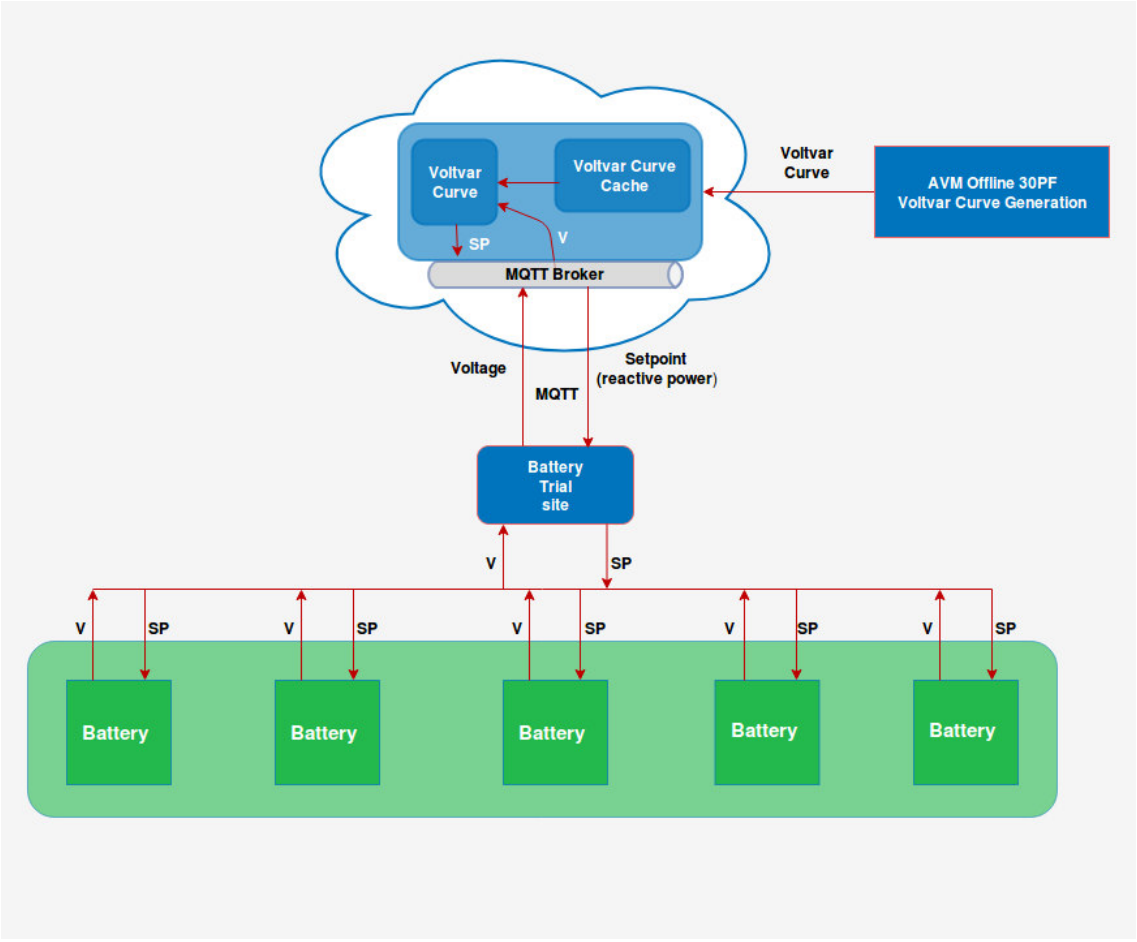

Figure 45: Data flow diagram for executing AVM in battery trials.

3.4.3.5 Tuning of AVM Algorithm to Specific Site

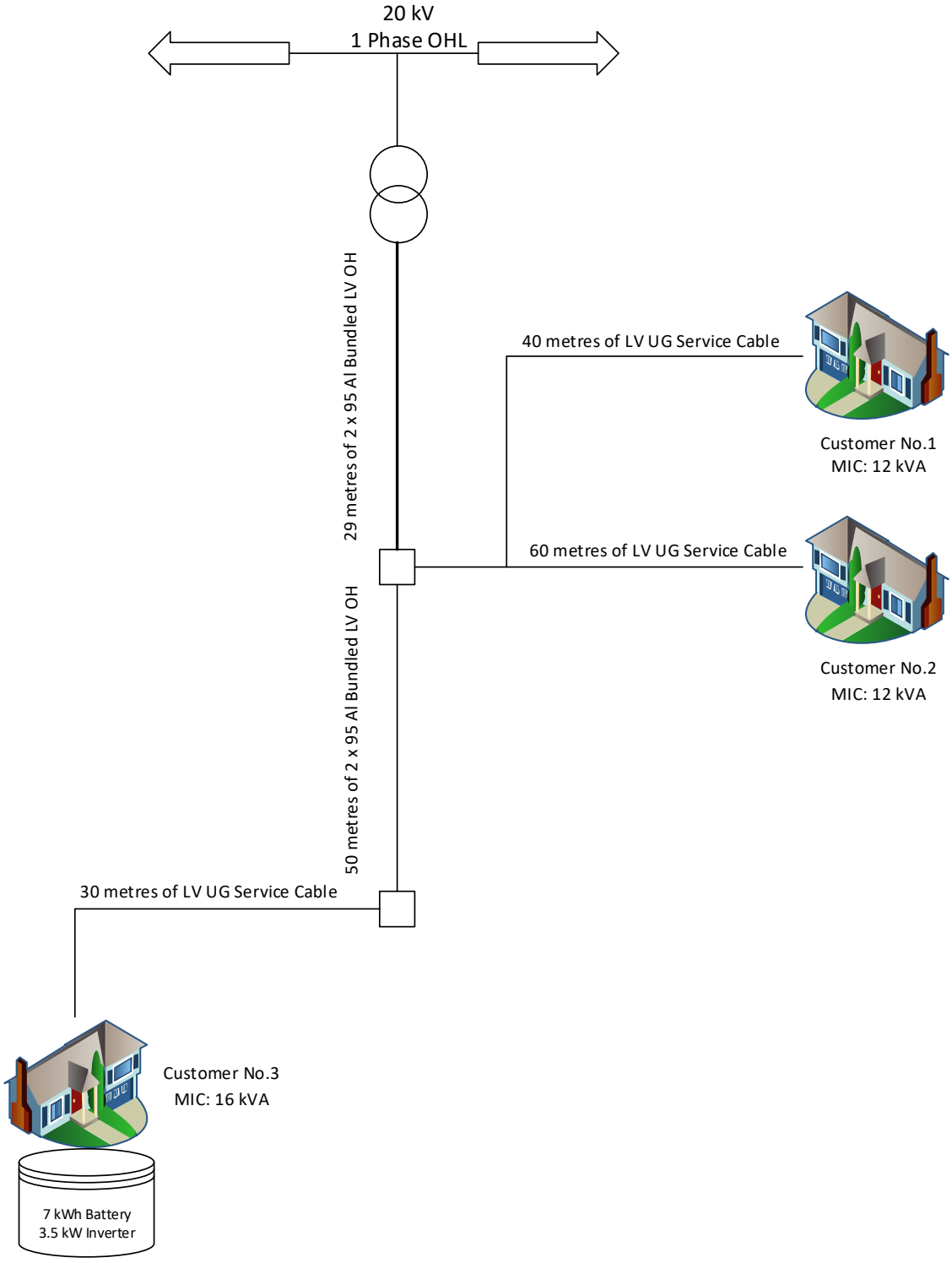

Figure 46: Single-line diagram of the small feeder at Killumney for installation of the inverter-based controllable devices.

3.4.3.5.1 Input Data and Assumptions

Battery Storage	LG Chem Li-Ion 7kWh
Battery Inverter	Solar Edge AC Coupling Inverter SE3500, 3.5 kW

Table 9: DER present at Killumney Battery Site

Figure 46 shows the single-line diagram of a small low voltage distribution system connected to the upstream system at Killumney. A battery storage system is connected to this sample system via an inverter. Characteristics of the inverters and battery are presented in Table 9.

Table 10 gives the system operation scenarios. In this table, Pbat is the power production of the battery. Coefficients of the ZIP load model are given by Z, I and P, for constant impedance, constant current and constant power components, respectively. Coefficient P can be found using P=1-Z-I. Load Factor (LF) determines the ratio of the active power consumption and the maximum power consumption presented in.

Scenario	Load Factor	P_{bat} /S_{bat}	Z	I	Power Factor
1	0.700	0.000	0.400	0.200	0.900
2	0.600	-0.250	0.400	0.200	0.850
3	0.500	-1.000	0.200	0.300	0.860
4	0.500	-0.750	0.200	0.300	0.870
5	0.500	-0.750	0.300	0.250	0.870
6	0.600	-0.500	0.300	0.200	0.850
7	0.600	-0.250	0.400	0.200	0.860
8	0.700	0.000	0.400	0.200	0.870
9	0.800	0.000	0.400	0.200	0.860
10	0.750	0.000	0.300	0.250	0.880
11	0.800	0.000	0.500	0.100	0.860
12	0.800	0.000	0.400	0.100	0.870
13	0.800	-0.250	0.400	0.200	0.880
14	0.800	-0.250	0.400	0.200	0.890
15	0.800	-0.250	0.500	0.150	0.900
16	0.800	-0.250	0.550	0.250	0.900
17	0.800	0.000	0.400	0.200	0.910
18	0.850	0.000	0.400	0.200	0.930
19	0.900	0.000	0.450	0.200	0.910
20	0.850	0.000	0.400	0.200	0.930
21	0.880	0.000	0.450	0.200	0.940
22	0.900	0.500	0.400	0.200	0.920
23	0.900	0.250	0.450	0.200	0.930
24	0.850	0.000	0.400	0.200	0.950

25	0.850	0.250	0.400	0.100	0.930
26	0.900	0.250	0.500	0.150	0.930
27	0.950	0.250	0.500	0.200	0.940
28	1.000	0.500	0.600	0.100	0.930
29	1.000	0.750	0.650	0.100	0.930
30	0.900	0.500	0.700	0.100	0.960
31	0.900	0.750	0.600	0.200	0.950
32	0.950	0.250	0.750	0.050	0.950
33	0.800	0.250	0.600	0.200	0.940
34	0.800	0.000	0.750	0.050	0.930
35	0.750	0.000	0.600	0.200	0.920

Table 10: Scenarios for RES-BAT-OV-0

3.4.3.5.2 VVCs of the network controllable devices for minimisation of the total loss

The second objective is considered here in order to apply the AVM algorithm for this trial site. The final VVCs for the battery storage as the controllable device in this trial site is presented in Figure 47.

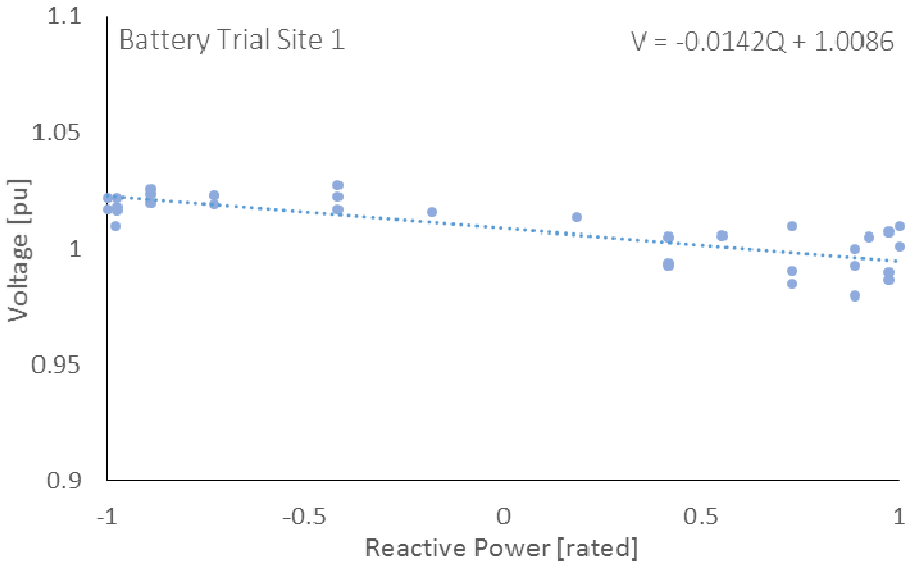

Figure 47: VVC of the battery storage for loss minimisation (m= -0.0142 (pu/kvar), c= 1.00862 (pu), Vopt= 1.00861 (pu)).

3.4.3.5.3 VVCs for the network RESs for minimisation of the voltage deviation from Vdesired=1 pu at load point

The second objective function is considered here for extracting the VVC using the proposed active voltage management algorithm in this study. For this trial site, the AVM algorithm suggests that all the inverters should inject the maximum available reactive capacity. It should be noted that in every possible scenario, the active power exchange of battery storage is determined by the availability of the corresponding source. With the objective considered in this

subsection, the inverters should fully dedicate their remaining capacities to provide positive reactive power support.

3.4.3.5.4 Summary of VVCs for this trial site

	Reactive power control mode		Voltage control mode
	m (pu/kvar)	**c (pu)**	**V_{opt} (pu)**
Energy Loss	Battery: -0.0142	Battery: 1.00862	Battery: 1.00861

Table 11: VVC characteristics for the PV array and battery storage in both modes of operation for RES-BAT-OV-0

Table 11 summarises the VVC for this trial site. It should be noted that these VVC is extracted with this assumption that the inverter is operated under reactive power control mode of operation.

Finally, it should be noted that if a VVC proposes reactive power support beyond the inverters' upper or lower limits, the reactive power support is set to the adjacent limit.

3.4.3.6 Performance of AVM Algorithm

In order to analyse the performance of the AVM algorithm for the Domestic Scale Battery site at Killumney it was necessary to extract data measurands from both the Battery inverter and the relevant secondary substation sensor. The deployment of a pole top secondary substation sensors for a period at a point adjacent to the dwelling before the AVM control technique was implemented allowed the recording of baseline network performance in the absence of AVM implementation. SERVO Live provided a straightforward interface for the extraction of these correlated datasets for external analysis. Figure 48 illustrates such measured data from this trial site including: Voltage, Active and Reactive Power at both the battery inverter and Secondary Substation sensor as displayed in the Servo Live dashboard.

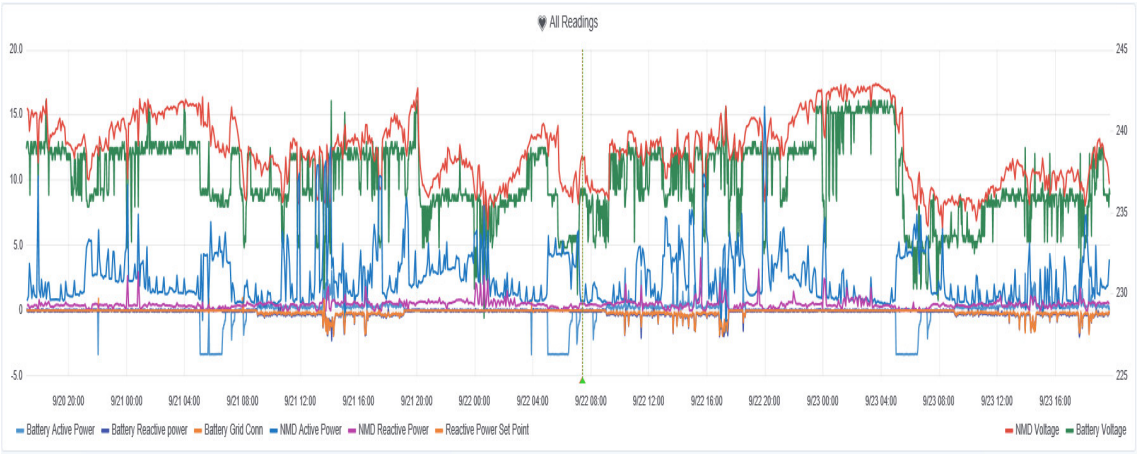

Figure 48: Measured data monitoring dashboard for Domestic Battery trial site

The assessment of the impact of the AVM algorithm necessitated the comparison of network performance in two scenarios, namely with and without the AVM control technique algorithm in operation. This comparison of electrical power imported from the upstream secondary substation is plotted in Figure 49, for both scenarios. Offline technical analysis of these data plots calculated that the introduction of the AVM algorithm effectively reduced the active power consumption at the point of connection by 8%. This reduction in energy loss is attributable to reductions in active power losses due to the optimisation of reactive power injections by the battery inverter.

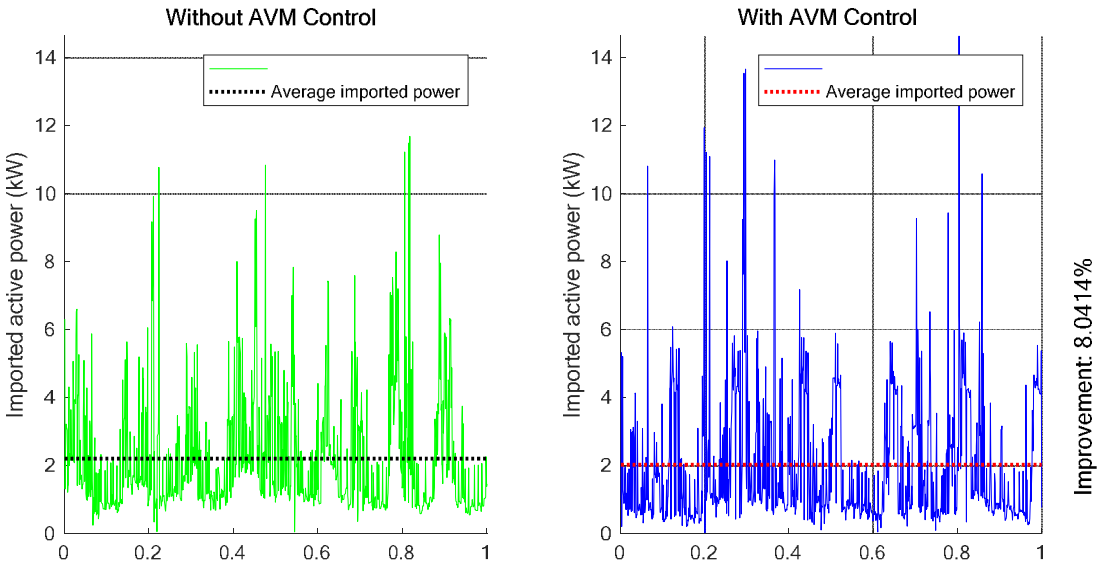

Figure 49: Performance evaluation of AVM algorithm for Domestic Battery trial site

3.4.4 Controllable Air Source Heat Pump (ASHP)

3.4.4.1 Background

Figure 50: Location of ASHP Trial site.

A key pillar of Ireland's decarbonisation strategy is to shift the heating of buildings away from traditional fossil fuel-based systems and towards electrified heat (eHeat). The predominant

technology for delivering eHeat is that of Air Source Heat Pumps (ASHPs). All moderns ASHPs are inverter based and therefore have the potential to provide system services to the distribution network through techniques such as those developed within the RESERVE project. A consequence of any shift towards eHeat is increased demand and stresses on the existing distribution network and a consequent increase in the value of system services such as those provided by the AVM control technique.

In identifying technologies to field test the control techniques developed in RESRVE ASHPs were identified as one of specific relevance given the expected increase in deployments both nationally and internationally. A test site was identified (detailed in section 3.4.4.2 below) and engagement with ASHP OEMs took place. Initial feedback from these engagements was positive with OEMs recognising that provision of system services by means of their devices' inverters could both create an additional revenue stream and potentially assist in lowering network constraints that could inhibit extensive ASHP deployment. Despite these positive indications the OEMs were unfortunately not sufficiently comfortable to allow third party control of the ASHP inverters at this time but continue to be open to such engagements in the future. Given the potential significance of ASHP control combined with the progress made in identifying and developing a site it was decided to proceed with the ASHP field trial albeit using a somewhat simpler Demand Side Management (DSM) based control trial rather than the AVM inverter-based trail originally planned.

3.4.4.2 Infrastructure Deployed

Figure 51: ASHP Units Installed at Youghalarra N.S.

A primary school located at Youghalarra N.S., Nenagh, Co Tipperary was identified as suitable field trial location for ASHPs. The school had undergone a deep retrofit with significant improvements in insulation and air tightness though upgrading of the building fabric. These improvements in the thermal efficiency of the building significantly increased the commercial viability of an ASHP deployment. This was achieved through the installation of cascaded 14 kW ASHP system in order to provide for all the building's space & water heating. The cascaded design allows the installation to most efficiently match the heating requirements at any point in time due to the fact a single ASHPs minimum load is generally limited to 30% of its rated capacity. The switch to ASHP based heating necessitated a significant upgrade to the school's electrical supply to that of a 29 kVA LV capacity which was implemented by the RESERVE

project. The additional hardware installed in order to implement Demand Response functionality at this trial site is described in Section 3.4.4.4 below.

3.4.4.3 Communications

The communications requirements for the ASHP trial site integration is based around the use of a public mobile network communications system that transfers readings for monitoring via MQTT to Servo Live and also to receive control messages to trigger the demand response mechanism.

3.4.4.4 Data Information Systems & Software

This trial site integration involves an equal mix of hardware and software components to both monitor and control the demand response aspects of the ASHP trial site. The hub of this integration is centred on an Arduino microprocessor with a connected current transducer clamp. This clamp measures the current readings in amperes and sends them to SERVO Live via MQTT for visualisation and analysis. The component relevant to the control of the ASHP from a demand response scheme involves the implementation of a single pole relay controlled by the Arduino microprocessor on the receipt of a control message via MQTT.

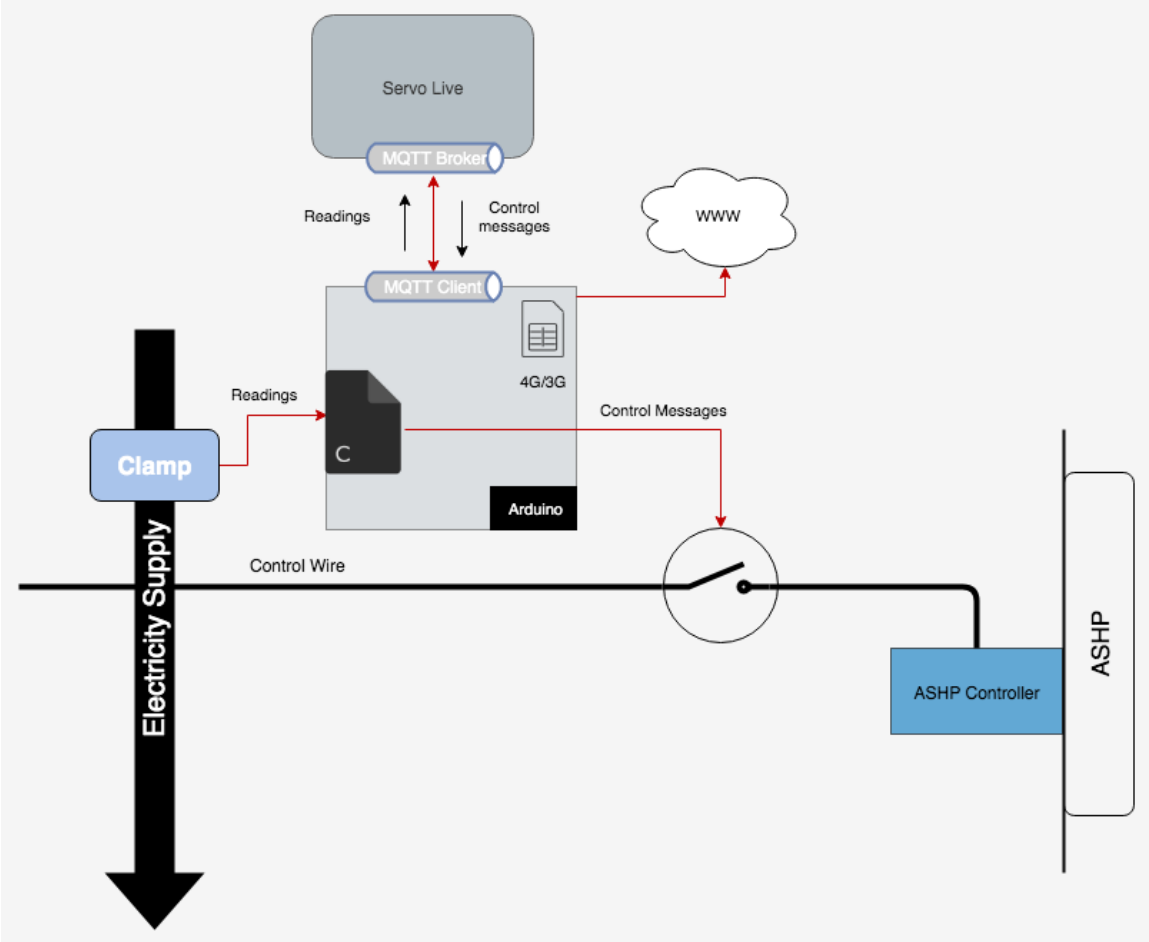

Figure 52: Communications Architecture of Controllable ASHP Trail Site

3.4.4.5 Performance of Demand Response Implementation

The impact of the Controllable ASHP on electricity demand at the school was assessed during a number of Demand Response tests. The tests were scheduled during periods of high demand by the ASHP system in order to understand the scale of the impact of this controllability. The output of these tests can be seen in Figure 53. Two distinct demand response events took place during the period displayed and these are indicated by the relay status signal marked in yellow in the graph.

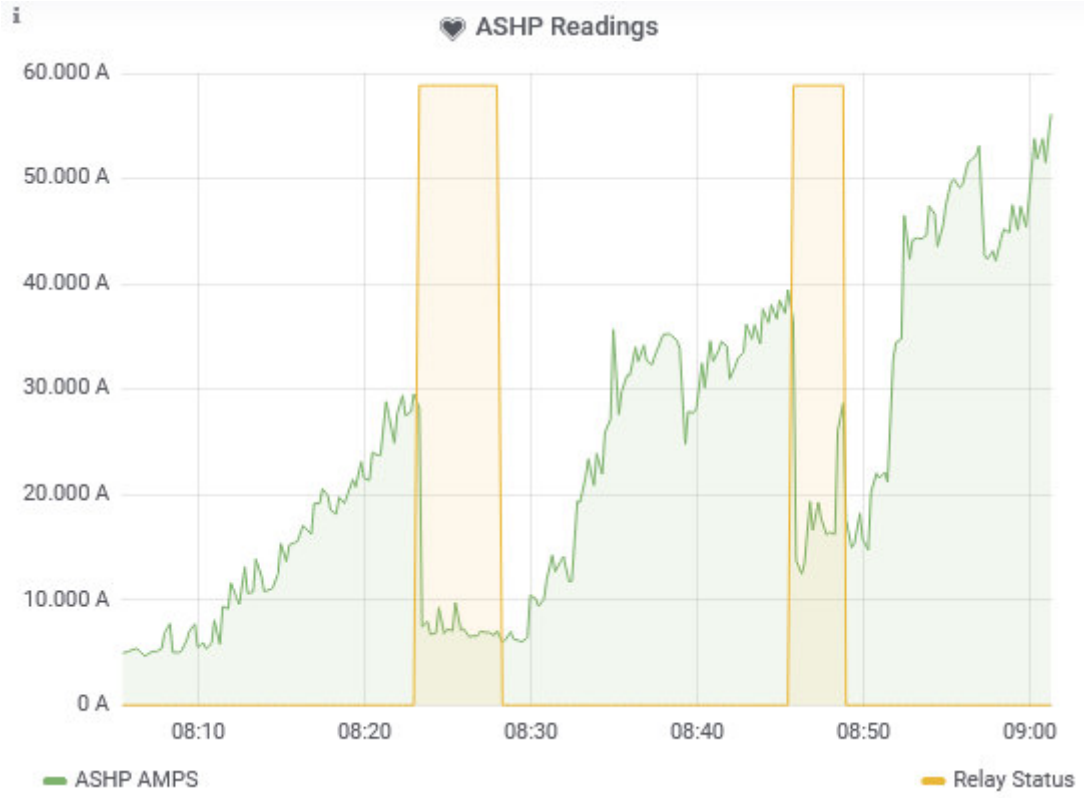

Figure 53: Impact of ASHP Control on Total Demand at Youghalarra National School

The magnitude of each demand response event can be quantified by examining the prior demand of the building and in this example the events equate to a response of 4.87 kW for a period of 7 minutes and 6.11 kW for a period of 5 minutes respectively.

Due to installation of a pole mounted secondary substation sensor, see Section 3.4.5, at the MV transformer to which the school is connected it was possible to view in real-time the impact of these demand response events on the local distribution network. This impact can be seen in Figure 54.

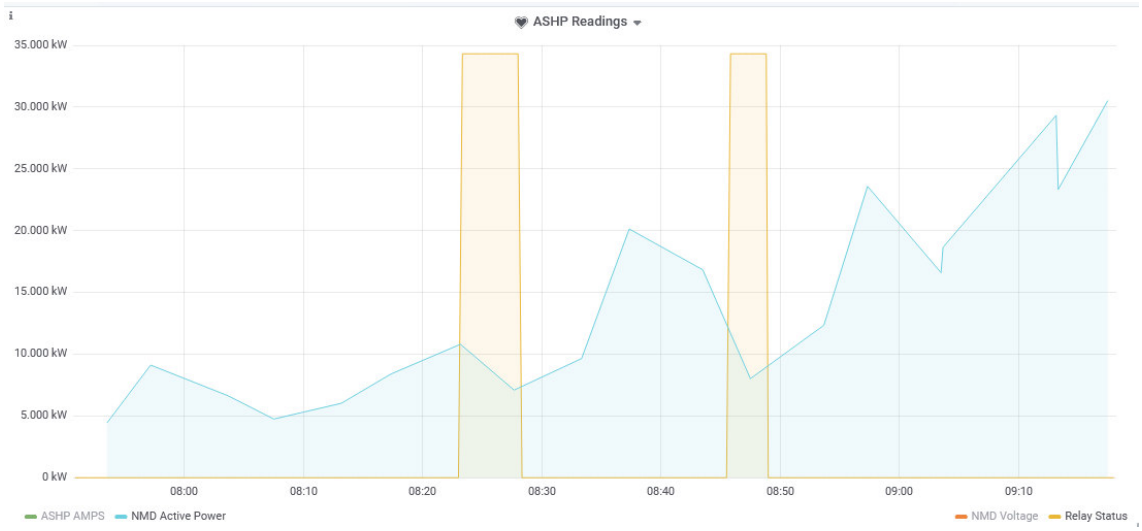

Figure 54: Impact of ASHP Control on Total Demand at Local Secondary Substation

The positive impact of the ASHP control on the loading of the local network is also evident here with reductions in demand of 34% and 52% recorded during the first and second Demand Response events respectively.

3.4.5 Secondary Substation Sensors

3.4.5.1 Background

The deployment and testing of DERs connected to the LV Network in Ireland provide an initial insight into the likely impact of the mass installation of distributed resources. In order to operate networks that have transitioned to such a structure it is necessary for DSOs to modify their monitoring regimes to include vision of lower voltage networks in addition to the higher (10 kV and above) voltages which have been the traditional focus of monitoring. This represents a fundamental inversion of the traditional focus of utility operators on larger scale, higher voltage infrastructure with singular patterns of power flow. The results of this focus can be seen in the number of substations with live metrics as per Table 12 below.

Name (V)	No. of Substations	Length of Network (km)	Observed
LV (400 / 230)	234,864	92,326	<1 %
MV +(10,000>)	795	105,793	99 %

Table 12: Observability on the Distribution Network in Ireland

In preparation for this transition to active LV distribution networks, ESB Networks has for several years been evaluating the evolution of compact, autonomous and affordable LV Network Monitoring devices capable of providing real-time vision. Working in co-operation with a number of OEMs, devices were adapted so that they complied with the specific requirements of Irish distribution networks and were capable of straightforward and safe installation without the need to disconnect any customers. An example of an LV Monitoring device deployed at the V2G Trial Site can be seen in Figure 55.

Figure 55: LV Monitoring Device installed at Ground Mounted Secondary Substation at the V2G Trial Site.

When scoping the RESERVE field trials, it was determined that it was necessary to validate the performance of the AVM control scheme in the field using equipment independent of the inverter-based device executing the control scheme. In addition, an ability to quantify the impact of the AVM scheme on the greater LV network beyond the DER device in question was desirable. It was therefore determined that the mass deployment of LV Monitoring Devices across the Field Trial sites was essential.

The deployment at scale of LV Monitoring Devices also presented an opportunity to field test the likely future scenario of third party owned and operated DERs. Whilst the field trials conducted in the RESERVE project were either directly developed by the DSO or consisted of deployments by an Aggregator working close co-operation with the DSO it is essential for the mass adoption of such technologies that such deployment can be independently realised by third parties. In such a scenario a new model of distributed monitoring is required, and the RESERVE field trial have also served to provide such a test in the real world.

3.4.5.2 Infrastructure Deployed

The relevant local secondary substations for the trial sites comprised a mixture of both Pole Mounted and Ground Mounted varieties. These are typical of the form of secondary substation found in rural and urban environments on the Irish distribution network.

The form factors of devices deployed can be seen in;

(i) Ground Mounted Secondary Substation, Figure 55.

(ii) Pole Mounted Secondary Substation, Figure 56.

Figure 56: LV Monitoring Device Installed on Pole Mounted Secondary Substation at the Trial Site at Youghalarra, Co. Tipperary.

The monitoring devices are capable of capturing performance data on the LV network including current, voltage, reactive and active power. The voltage at the secondary substation is measured by direct coupling of the device to the LV busbar of the secondary substation by means of a Drummond clamp with fused Hartling socket see Figure 57.

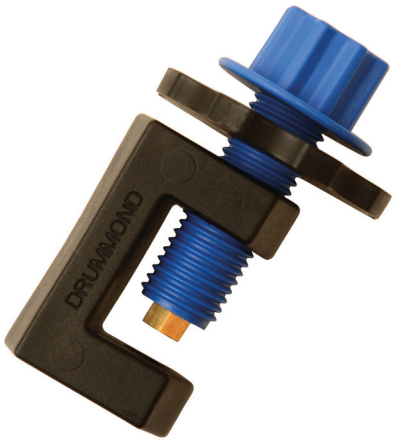

Figure 57: Drummond Clamp with Fused Hartling Socket

The monitoring devices use Rogowski Coils to measure the AC current of feeders at the secondary substation see Figure 58 for sample. The Rogowski Coil is a flexible current transformer which measures AC current. The Rogowski Coil is a toroidal coil, the output of the coil is a voltage signal proportional to primary current. The coil is a rope-style CT that physically wraps around the conductors of the feeder requiring monitoring. Rogowski coils are installed as they provide a versatile solution where space is limited and can be installed around live feeders without interrupting supply. They provide a significant advantage over traditional CTs as the risk of overloading of the transformer due to an open-circuited CT is eliminated.

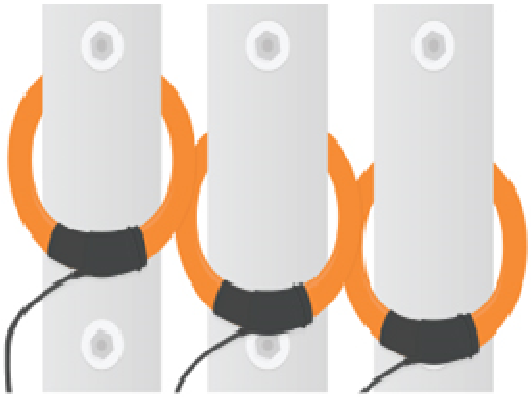

Figure 58: Illustration of Rogowski Coils on a 3 Phase Feeder

3.4.6 Verification of Network Codes

The delivery of field trials in Ireland succeeded in implementing and validating the AVM Control technique. In addition, the field trials served to validate several Network Code proposals developed in the RESERVE project under real-world conditions. The Network Code proposals which were successfully validated in the Irish Field Trials are detailed below;

NC. 14: Decentralised Voltage Control

The implemented trial sites deployed a mixture of centralised and decentralised control architectures. The flexibility afforded by this menu of options allowed for the customisation of solutions for each trial site technology. The domestic scale battery trial sites, at which the inverter-based equipment was owned by a commercial aggregator, were better suited to a centralised control scheme which allowed the AVM control scheme to be implemented in the cloud and avoided the installation of additional equipment locally at each site. In the case of the V2G trial site the relative immaturity of the device's control hardware necessitated the deployment of additional hardware locally to the device in order extract measurands and apply AVM mandated set-points. This local hardware implementation also facilitated the AVM control scheme to be implemented at the device itself where it operated independently of external control thus implementing a decentralised architecture. This implementation proved effective in applying the AVM control technique and successfully demonstrated the implementation of decentralised voltage control in a real-world environment.

NC. 18: Reactive Power Capability of Distributed Generators

The permitted range of power factors for all devices, other than Wind Turbines, connected at Distribution Voltages is currently restricted to lagging power factors only. In Ireland this range is currently mandated as falling between 0.95 lagging and unity. This restricted range evolved from the traditionally correct assumption that all domestic and industrial loads are fundamentally inductive in nature. The technologies deployed at the RESERVE trial sites have a considerably greater performance range than traditional devices however and are thus capable of the controlled implementation of leading power factors.

The implementation of leading power factor was successfully implemented at RESERVE trial sites when mandated by the AVM control scheme. The successful implementation of a leading power factor can be viewed in Figure 59 which details the Voltage and Reactive Power performance of the inverter at the Killumney Domestic Scale Battery trial site. In the period between 12:54 and 12:58 the Voltage recorded at the trial site can be seen to fall from a stable 237 V to a nadir of less than 228 V. During this same period the AVM controlled inverter adjusted Reactive Power output to a point where the device exported Reactive Power. The generation/export of Reactive Power, with export value peaking at greater than 2 kvar, equates to a power factor 0.80 leading. The net impact on system Voltage can be seen in the rapid recovery of the voltage, with system voltage returning to 237 V by 13:10, following the implementation of a leading power factor.

Figure 59: Voltage and Reactive Power Performance at Killumney Battery Trial Site

4. Conclusions

In this deliverable, the activities undertaken to conduct the Dynamic Voltage Stability Monitoring field trial is explained. Results and analysis obtained from the in-field experiments are documented and these results validate the proposed network codes.

For the validation of DVSM technique, a hybrid inverter prototype was developed and tested at RWTH. Field tests were performed with the Irish grid where the grid impedance was measured up to 1 kHz. The proposed impedance measurement device enables grid operators to measure impedance in real-time and additionally perform the non-parametric impedance-based stability criterion developed in RESERVE.

Based on field experiments and real-time simulations, we have firmly validated the following network codes:

- NC.14 Decentralised Voltage Control
- NC.18 Leading Power Factor Operation
- NC.17 Dynamic Stability Margins
- NC.15 Requirements for new behaviour of RES inverters
- NC.16 New requirements for the perturbations injected from RES inverters

The Irish Field Trials also proved successful in demonstrating the complete end to end realisation of the AVM Voltage control technique in numerous real-world scenarios. The realisation of this success demonstrated the viability of all elements of the trials incorporating, the delivery of relevant DER infrastructure; tuning of the AVM algorithm for specific site conditions and objectives; the integration of trial site technologies into a number of distinct ICT communications architectures; the implementation of a business model incorporating a commercial aggregator and the delivery of a network monitoring solution capable of verifying the control technique's implementation.

The AVM control technique algorithm proved itself flexible and capable of providing a menu of optimisation solutions across a range of network topographies containing a broad mixture of DER technologies. The collation of the detailed data required to be inputted into the algorithm proved to be somewhat cumbersome as system records at LV are historically less detailed and robust than those recorded for infrastructure rated for higher voltages. Nevertheless, the AVM control technique proved itself robust through its capability to achieve the desired objective of network performance despite the degree of uncertainty regarding the submitted baseline parameters. In the case of the Solar PV trial in particular the algorithm demonstrated its capability to determine an optimised VVC in a scenario where multiple independent sources of generation were present on the immediate local network. This scenario is redolent of the likely future configuration of substantial portions of distribution networks and indicates the feasibility of the AVM Control technique to support same.

The field trials built on the initial implementation of Voltage control through the introduction of additional energy system actors which allowed for the realisation of an alternative model of implementation. Collaboration with a commercial aggregator in the case of the domestic scale battery sites allowed the trials to expand to additional locations. By leveraging this commercially deployed infrastructure we were able to expand the scale of the trails at minimal cost to the project as the cost of the of the battery hardware, installation and communications solution costs was borne by the aggregator. The expansion of the trials which was achieved in this manner can serve as a template for what is achievable when multiple market actors are engaged in the provision of voltage control services. This success highlights the requirement for suitable market mechanisms to be established so that what has been proven implementable can also be made commercially viable.

From the perspective of the trial site implementation of the algorithms and monitoring during the trials it was noticed that there are significant barriers to the implementation of such concepts centred around the diversity and capabilities of the inverters and interfaces available at the edge of the network. These interoperability factors came in many forms including communication

capabilities, low level configuration access, vendor specific factors like vendor lock in and 3rd party platform integration factors. All the trials detailed in section 3.4 carried separate interoperability factors and that were overcome by creating generic software components, like the execution of the Active Voltage Management algorithm, and using containerisation to allow its deployment in a wide range of scenarios. These scenarios, in the context of the RESERVE project, entailed the deployment of the solution to bespoke hardware devices at the edge of the network in the case of the V2G trial, cloud platforms, like SERVO Live, in the case of the Killumney Battery trial and directly to the inverter in the case of the Solar PV trial. While the goal of the trials was to ultimately deploy and test the concepts to live devices, the performance of these concepts and their impact on the grid needed to be assessed and the carrying out these assessments was subject to the same interoperability factors as the execution of the algorithms. To overcome this a containerised implementation of an MQTT broker was integrated into SERVO Live and containerised MQTT clients were deployed to the edge devices at the trial sites and the network monitoring devices to gather and send the power system readings, algorithm derived set points and device status to SERVO Live for storage and visualisation.

In addition to the implementation of the AVM control technique itself the trials also served to demonstrate the systems and infrastructure necessary to implement transformed distribution networks incorporating intelligence, controllability and real-time vision at LV. Central to this was the successful mass deployment of Secondary Substation Sensors across the trial sites and their integration in a standardised manner into SERVO Live platform. The sensors were successfully integrated into both ground mounted and pole top secondary substations. These rapid deployments were achieved without network outages impacting existing customers highlighting the relative of ease with which they can be further scaled. The mass deployment of these sensors also served to demonstrate the viability of a new format of electricity network architecture which is necessary to accommodate an array of emerging business models.

In summary the AVM Voltage Control trials demonstrated that the solution can be implemented in real world scenarios, is inherently scalable, can be integrated with additional external monitoring devices and is capable of positively contributing towards the resolution of constraints encountered by the distribution network.

ANNEX 1 Performance of AVM Algorithm at V2G Trial Site

In order to validate the proposed active voltage management technique, the minute by minute active and reactive power demands at all load points and also the other required data are modelled in a set of minute by minute scenarios for one week and for each minute a three-phase unbalance power flow has been conducted to find the three-phase voltages and currents and therefore, the network losses. The bottom-up demand-model (see D3.2) is once again utilised to generate a week-long demand profile for the customers in this LV feeder. In the load profile the active power consumptions at the PCCs are also taken into account.

At the first stage, in three separate studies, three different fixed power factor operation strategies are assumed for the V2G system connected to this low voltage distribution system, i.e., 0.95 inductive, 1 and 0.95 capacitive. These settings constrain the reactive power support of each V2G inverter to absorb roughly one-third of the value of active power consumed by the V2G charger, zero and inject about one-third of the value of active power consumed by the V2G charger. A fixed power factor is typical control approach for an inverter-based controllable device connected to a low voltage distribution system to reduce the voltage-rise effect caused by the excessive active power injections.

The operation of the set-points extracted using the VVC are compared to the operation at the aforementioned fixed power factor strategies. For this study, in the week-long time-series power flows, the V2G system on this LV feeder is tasked with following its assigned VVC presented in the previous sub-section.

The operational constraints of various types of inverter-based RES were analysed in D3.3. In this subsection different limitations that may be applied in order to ensure the safe operation of the inverter and also an acceptable level of power quality will also be applied and the obtained results are compared to those obtained with the case that the capacity constraints are considered as the only constraints for operation of the system inverter (V2G charger) and also the results obtained under those three fixed power factor assumptions that were mentioned before.

Figure 60 shows the range of variations of total active power demand absorbed from the upstream system through the step-down transformer of this system. The active power consumption of the V2G system is also depicted in this figure for the week-long time-series simulation. These active power consumptions have been normalized so that the peak load value is equal to Load Factor (LF) 1. The values of Power Factor (PF) are also provided in this figure. Using these values and normalized active power consumptions, one can reach the normalized reactive power consumptions. All the sub-plots of Figure 60 are provided for the most probable weekly scenario.

The component of every demand customer is compartmentalised into constant impedance, constant current and constant power. The components of the adopted ZIP load model are also presented in Figure 60. This ensures a realistic scenario and represents the voltage dependence behaviours of the system loads as those that can be seen on practical low voltage distribution system. In this figure, “Z” and “I” introduce the constant impedance and constant current shares in the load model in percent. The constant power share can be easily found (100-Z-I).

The observed voltage measurement at the terminal of the V2G system is mapped to its set-point operation of reactive power based on the explanations provided on the application of the AVM algorithm. The results of these simulations are briefly discussed in this subsection.

Figure 60 also shows the active power injected by V2G system. In order to present the values of the reactive power injection of the inverter, it has been assumed that the inverter is tasked with following the VVC provided in the previous subsection. The maximum capacity and also minimum power factor limitation restrict the maximum reactive power that the inverter can inject into the system at PCC. The minimum power factor of the inverter ensures the safe operation of the inverter and limits the harmonic distortions. This parameter is provided by the manufacturer.

For this V2G converter the minimum power factor of 0.8 has been recommended by the manufacturer.

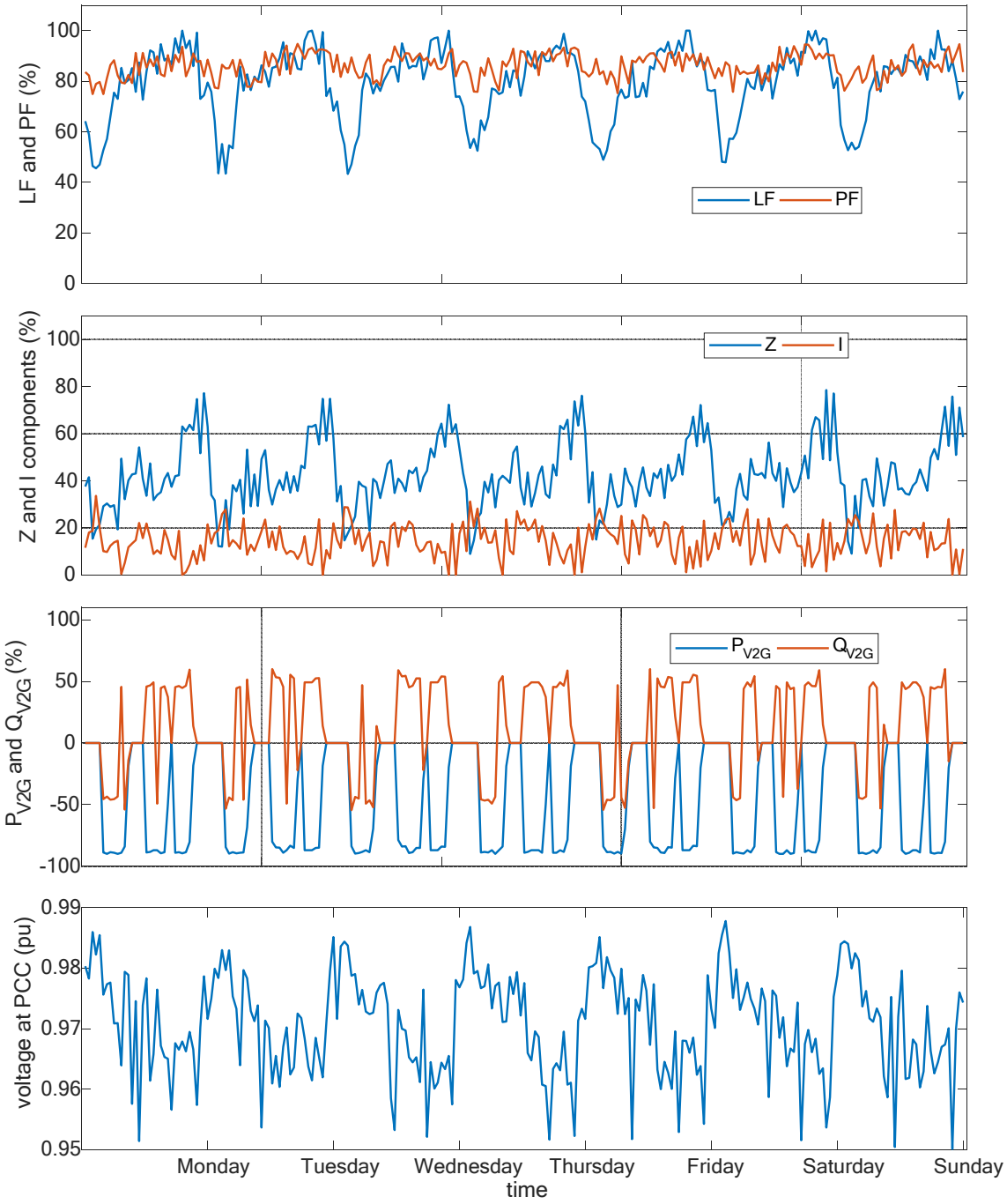

Figure 60: Total active power demand at system load buses, load power factor, active/reactive power injections of V2G system, ZIP components at system load buses and voltage at PCC.

Table 13 summarizes the performance metric of interest for the time-series power flow simulation utilising the VVC found in the offline-analysis for loss minimization (see the previous sub-section). The results are also presented for the fixed power factor scenarios. As can be seen in Table 1 1, under loss minimization as the objective, the proposed decentralized AVM algorithm reduces the weekly energy loss by about 8% compared to the best energy loss found under the fixed power factor assumption. The definition of the performance metrics was provided in D3.3.

Table 13 presents the results obtained in the implementation of the VVCs for AVM considering two different set of constraints on operation of the inverter of the V2G system to show the effects of constraints on the effectiveness of proposed AVM algorithm. According to Table 13, with the accurate constraint modelling, the results of applying the proposed AVM algorithm for optimising the reactive power dispatch to minimise the weekly energy losses are even better than the case with capacity constraint as the only constraint on the operation of the system inverter. It may seem a little bit surprising, but was best explained in D3.3.

Objective		Total Energy Loss (kWh)
Min. Power Loss with inverter capacity constraint as the only limitation [kW]		193.835
Min. Power Loss with accurate operational constraints (capacity constraint and power flow constraint)		**192.880**
Min. Power Loss [kW] Current NC recommended Lagging PF>0.92		200.585
Fixed Power Factor	0.95 Lag Power factor	208.153
	Unity Power factor	208.852
	0.95 Lead Power factor	211.021

Table 13: Comparison of active power loss metrics for all cases

5. List of Abbreviations

AC	Alternating Current
ADC	Analog-to-Digital Converter
API	Application Programming Interface
ASHP	Air Source Heat Pump
AVM	Active Voltage Management
BAU	Business as Usual
CHAdeMO	CHArge on de Move (A DC for Fast Charging Protocol for Electric Vehicles)
DC	Direct Current
DER	Distributed Energy Resource
DQ	Direct-Quadrature
DSM	Demand Side Management
DSO	Distribution System Operator
DVSM	Dynamic Voltage Stability Margin
eHeat	Electrified Heat
ESB	Electricity Supply Board
FIFO	First In, First Out
FFT	Fast Fourier Transform
FPGA	Field Programmable Gate Array
GIS	Gas Insulated Switchgear
HiL	Hardware in the Loop
ICT	Information & Communications Technology
IPM	Intelligent Power Module
KPI	Key Performance Index
Li	Lithium
LPWAN	Low-Power Wide-Area Network
LV	Low Voltage (< 10 kV)
MQTT	Message Queuing Telemetry Transport
MV	Medium Voltage (10 kV – 38 kV)
NI	National Instruments

N.S.	National (Primary) School
NTC	National Training Centre
OEM `	Original Equipment Manufacturer
OPF `	Optimised Power Flow
OpenFMB	Open Field Message Bus
PCC	Point of Common Coupling
PF	Power Factor
PRBS	Pseudo Random Binary Sequence
p.u.	per unit
PV	Photo-Voltaic
RWTH	Rheinisch-Westfälische Technische Hochschule
SERVO	System-wide Energy Resource & Voltage Optimisation
SSAU	Secondary Substation Automation Unit
V2G	Vehicle to Grid
VOI	Virtual Output Impedance
VVC	Volt-var Curve
WFZ	Wideband-frequency Grid Impedance
WSI	Wideband System Identification

6. List of Figures

7. List of Tables

8. Bibliography

[1] S. K. Gurumurthy, M. Cupelli and A. Monti, “A Generalized Framework for Synthesizing Virtual Output Impedance Control of Grid Integrated Power Electronic Converters,” in *2018 IEEE International Conference on Power Electronics, Drives and Energy Systems (PEDES)*, 2018.